Multi-Wire Proportional Chamber (MWPC)

MWPC ...

substantial functionality improvement
due to cathode strips/pads ...

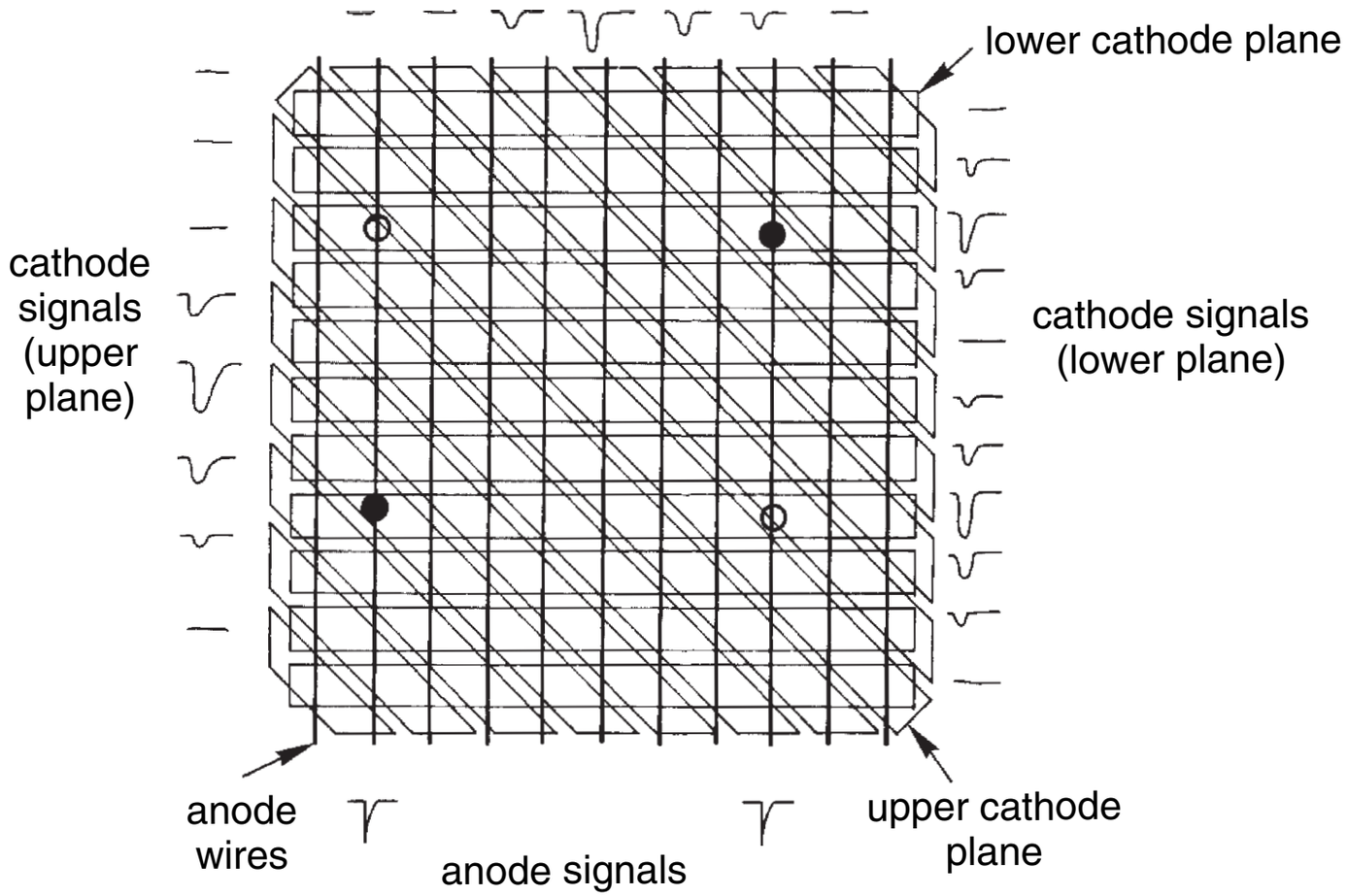

Cathode readout yields:

- 2-dim. information
  true 2d: use pads ...
- high spatial resolution
  due to center of gravity reconstruction
- resolving ambiguities
  using second strip pattern or pads

Can wires be avoided?

Micro-strip Gas Chambers (MSGC)

Can one avoid wires?

Anode realized via microstructures on dielectrics ...

Simple construction (today)
Enhanced stability & flexibility
Improved rate capabilities

First MSGCs developed in 1990ies ...

Problems: charging of isolation structure
[➛ time-dependent gain; sparks, anode destruction]

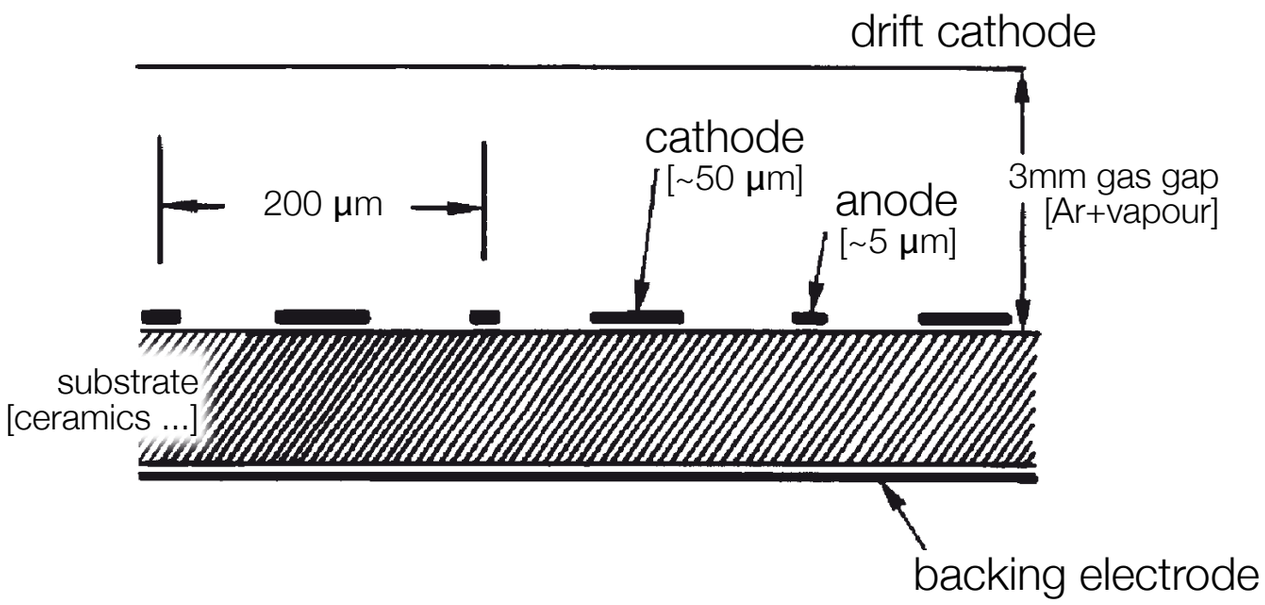

Schematics of MSGC field lines

high field directly above anode
ions drift only 100 µm; yields low dead time ...

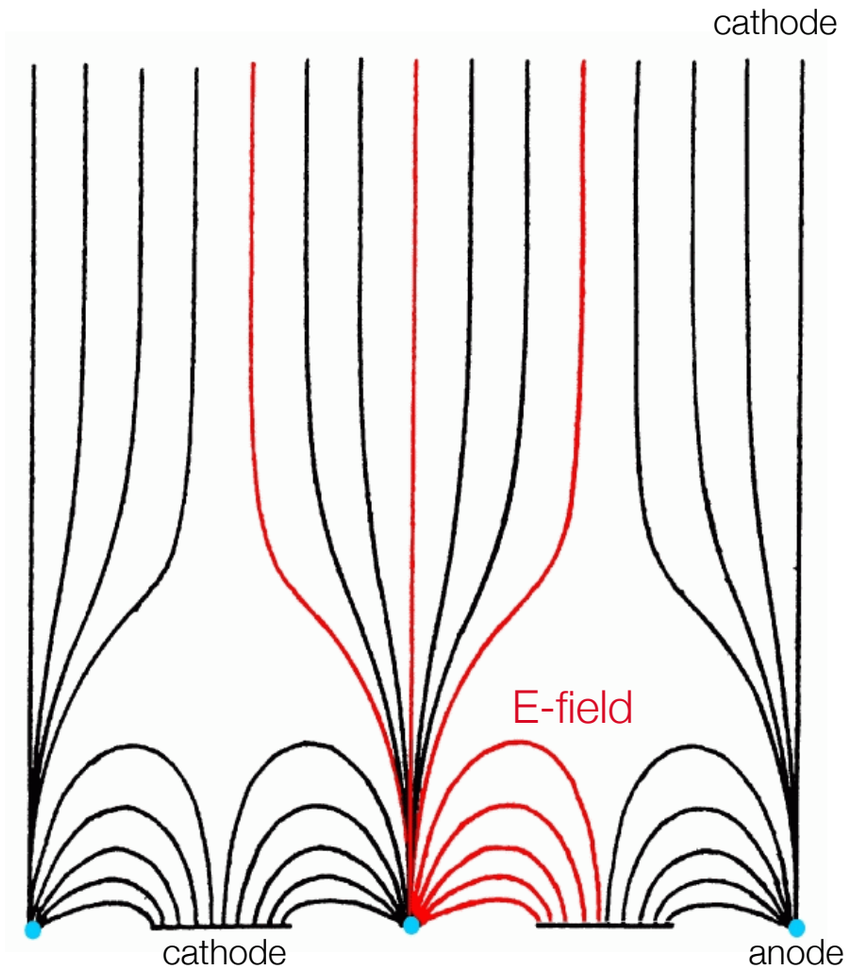

Micro-strip Gas Chambers (MSGC)

MSGCs prone to aging problems ...
Solution: intermediate grid ...

e.g.: Micromegas
GEM detectors [Sauli, 1997]

Micromegas:

Fine cathode mesh collects ions
still fast; no wires ...

GEM (Gas Electron Multiplier):

Thin insulating kapton foil
coated with metal film ...

Contains chemically produced
holes [100-200 μm]

Electrons are guided by high
electric drift field of GEMs ...

Avalanche production ...

Electrons drift to anode
GEM collects ions

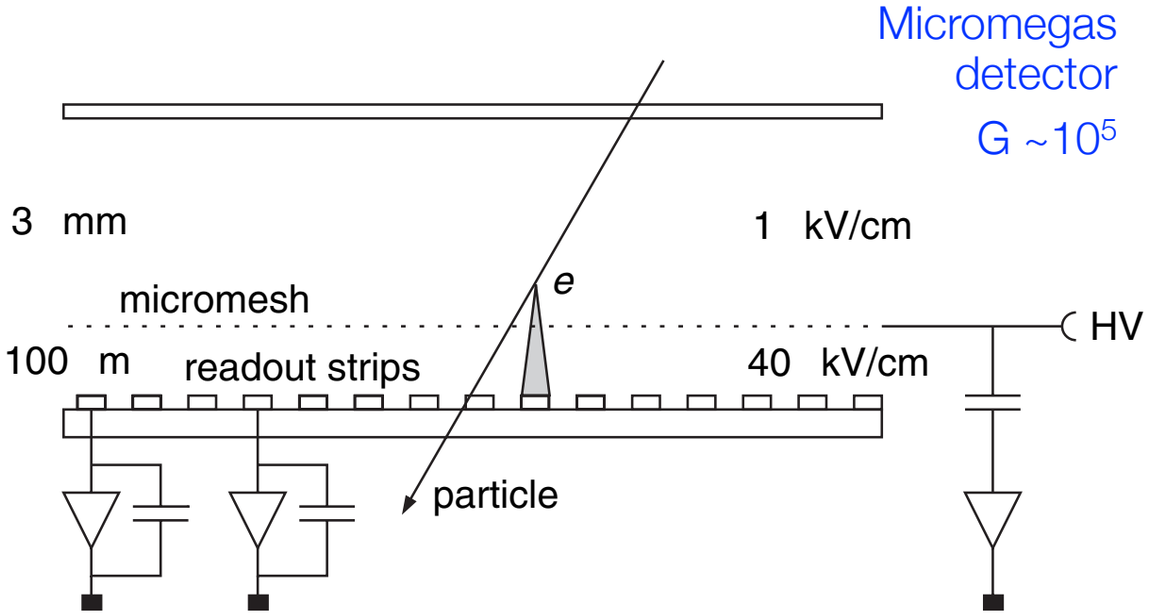

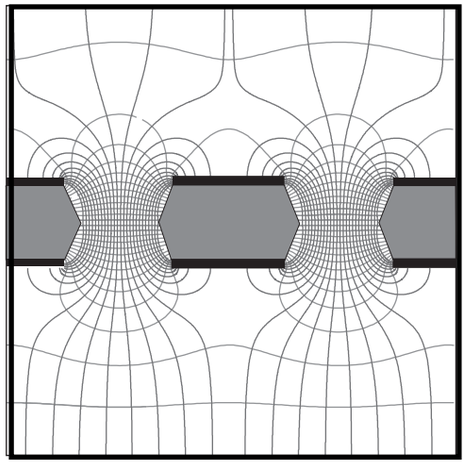

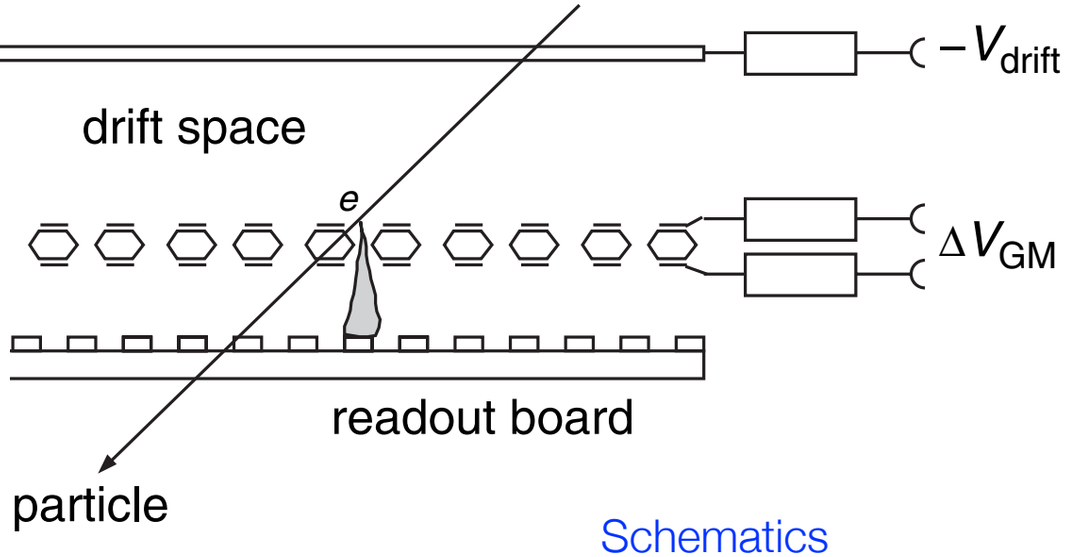

Schematics
of GEM detector

Micro-strip Gas Chambers (MSGC)

GEM

Gas Electron Multiplier

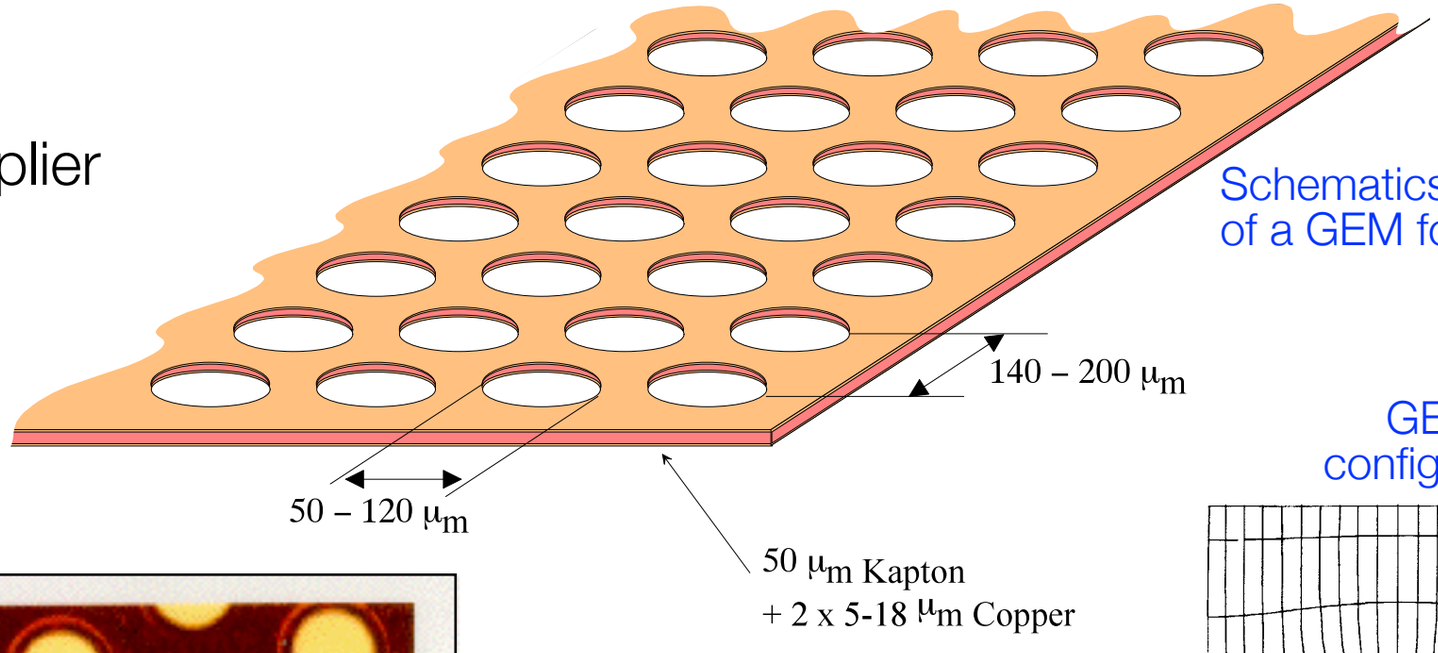

Schematics of a GEM foil

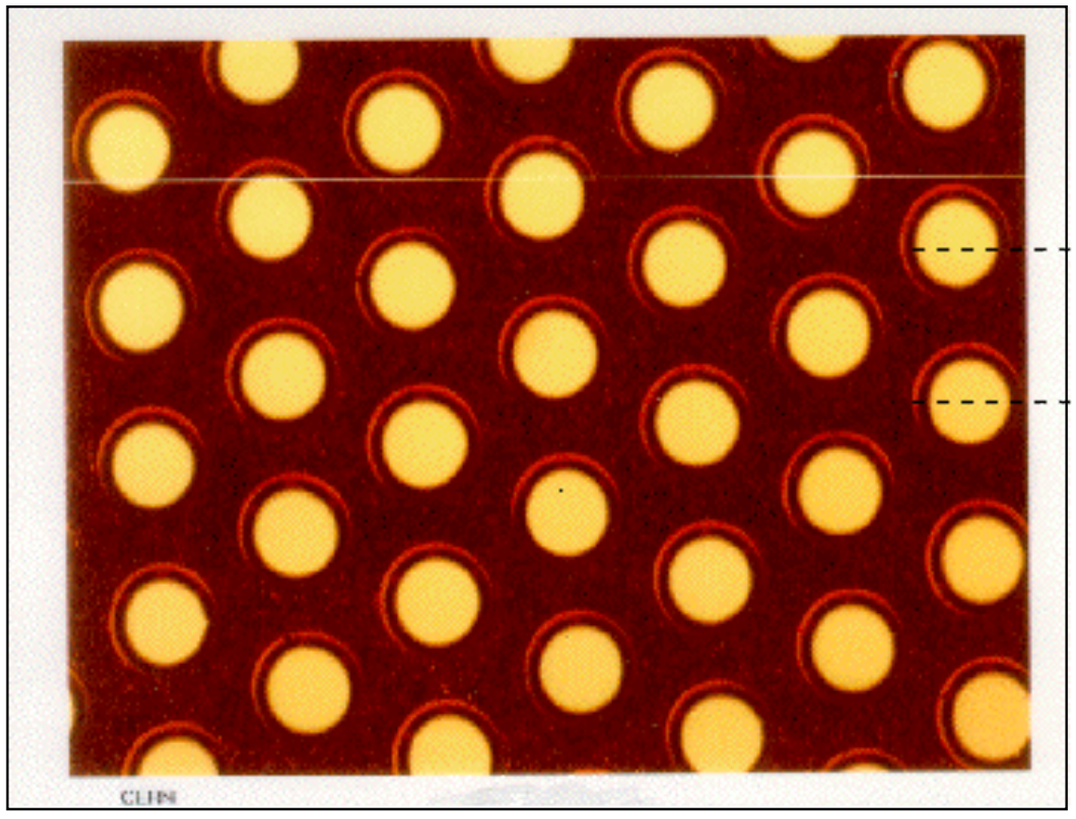

Micro photo of a GEM foil

GEM field configuration

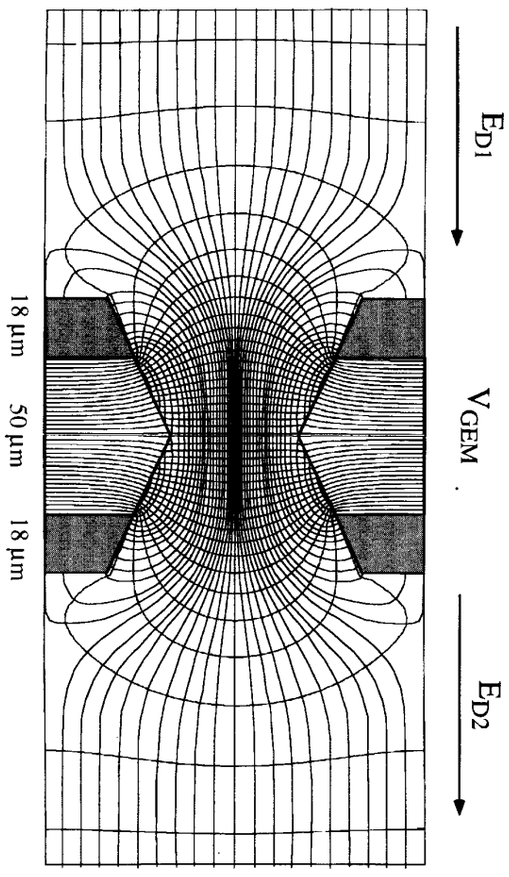

Ionization Chambers – Signal Shape

Pulse mode operation

derive signal for single ionizing particle [R = ∞]

$$W = {}^1\!/_2\, CU^2 = {}^1\!/_2\, CU_0^2 - N\int_{z_0}^{z_f} qE_z dz$$

$$= {}^1\!/_2\, CU_0^2 - N_+q_+\,\frac{U_0}{d}\,(z_+ - z_0) + N_-q_-\,\frac{U_0}{d}\,(z_- - z_0)$$

$$U = U_0 + \Delta U \qquad U^2 = U_0^2 + 2\Delta U\, U_0 + \Delta U^2$$

$$\Delta U = -\frac{N_+q_+}{Cd}(d - z_0) + \frac{N_-q_-}{Cd}(0 - z_0) = \Delta U_- + \Delta U_+$$

$$= -\frac{N}{Cd}\,[e(d - z_0) - e(0 - z_0)] = -\frac{Ne}{C}$$

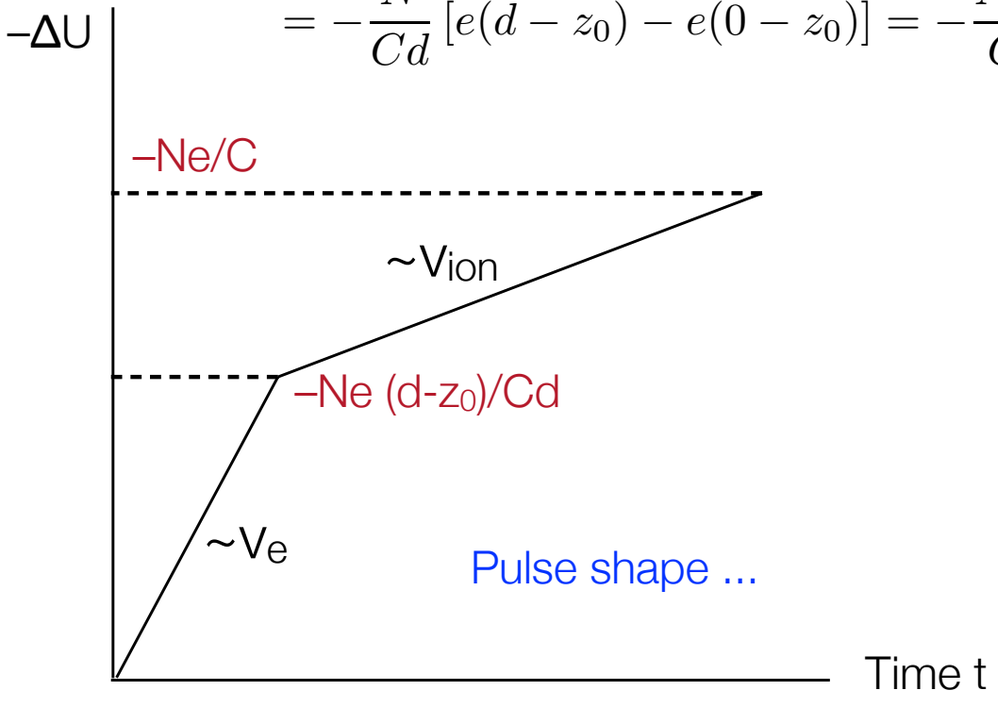

Pulse shape ...

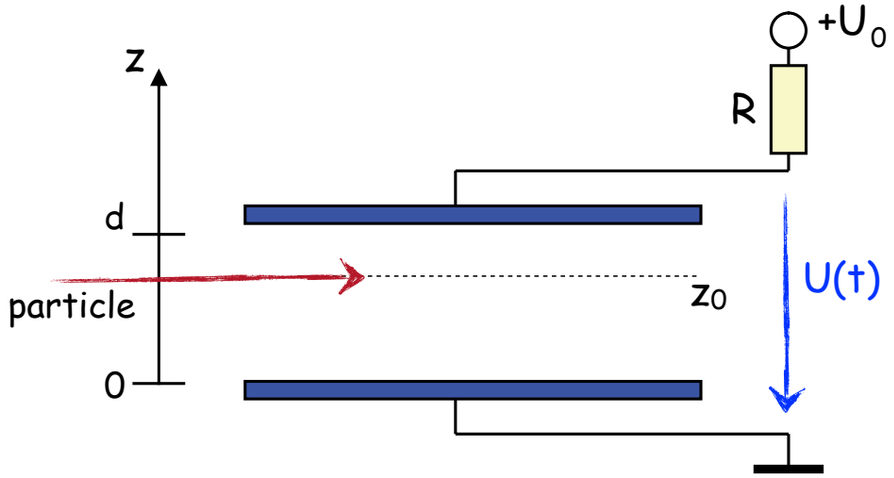

Schematic view of an ionization chamber

Final signal independent of ionization position and of detector dimension ...
[see also Geiger counter]

Time evolution of pulse height:

$$z(t) = v_D \cdot t$$

$$\Delta U = -\frac{Ne}{Cd}\left(v_D^{\mathrm{e}} + v_D^{\mathrm{ion}}\right) t$$

with:

$$v_D^{\mathrm{e}} \approx 1000 \cdot v_D^{\mathrm{ion}}$$

Typical:

$v_{d,e}$ = 4 cm/μs
$v_{d,ion}$ = 4 cm/ms

Ionization Chambers – Signal Shape

Schematic view
of an ionization chamber

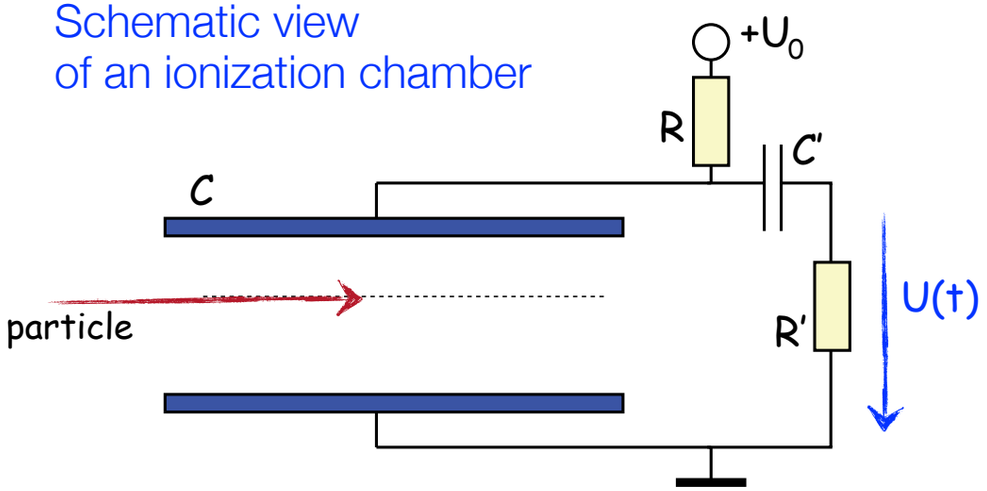

Pulse shape
with RC circuit ...

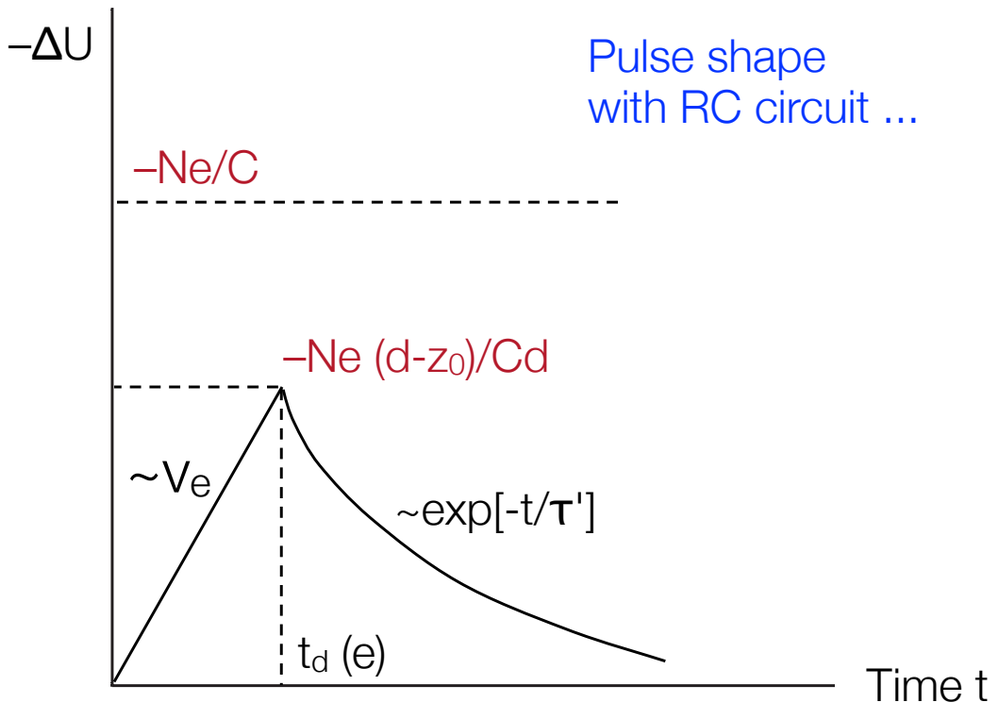

Pulse mode operation
[Use RC circuit; R finite]

Response time of chamber: $\tau = RC$

Must be sufficiently large with respect to t_{signal}

Example: 2 x 2 x 10 cm^3 chamber

Electron drift time: $t^-_{max} = d/v_{d,e} = 2cm/4cm/\mu s = 500$ ns
Ion drift time: $t^+_{max} = d/v_{d,ion} = 500\ \mu s$

Suppress ion signal by C'R' high pass filter
with time constant $\tau' = R'C'$

Chose: $t^-_{max} < \tau' < t^+_{max}$

Ex.: τ' $= 1\mu s$
C $= 1pF$, R $= 10M\Omega$
C' $= 1pF$, $C_{tot} = CC'/(C+C') = 0.5$ pF
R' $= \tau/C = 1\ \mu s/0.5$ pF $= 2\ M\Omega$

Features:

linear rise; exponential fall
dead time $T_{dead} \approx \tau'$
position dependent pulse height
position dependent resolution

Ionization Chambers – Frisch Grid

Removal of
position dependent signal ...

[O. Frisch, 1944]

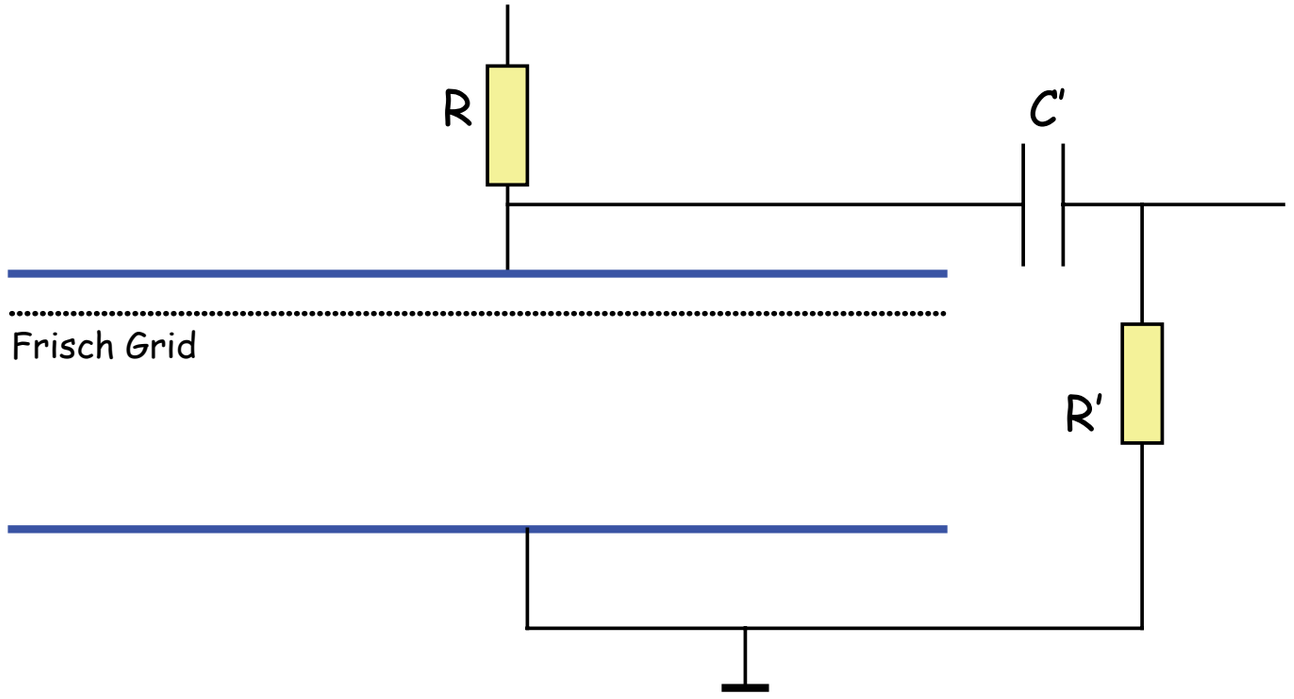

Principle:

Introduce wire plane
at intermediate potential ...

Shielding of induced charges
Wire plane transparent to electrons

Signal on anode only generated
by electrons that have passed the Frisch grid

All electrons appear at the same distance
thus: no position dependence ...

Difficulty: Small signals ...
Need sensitive, low-noise pre-amplifiers ...

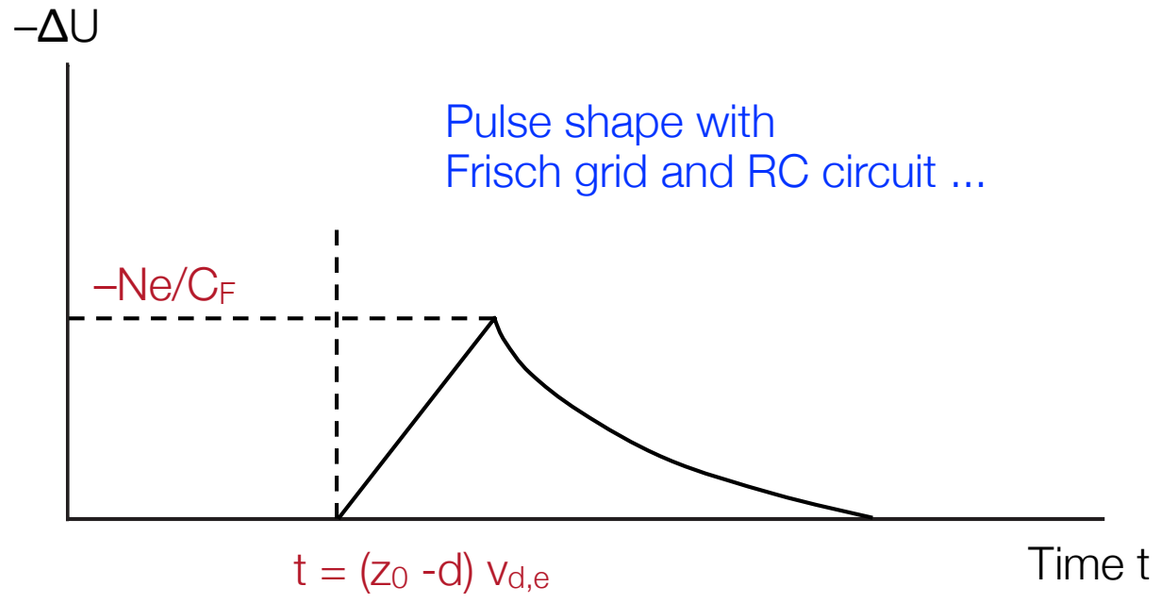

Ionization Chambers – Music II

Parameters:

gas	P10 (Ar/Methan 90/10)
pressure	1 atm
active area	102 x 60 cm^2
depth	51 cm
electric field	150 V/cm
potential	9 kV
ionization	70 Z^2 pairs/cm
drift velocity	5 cm/µsec

Fragment charge spectrum

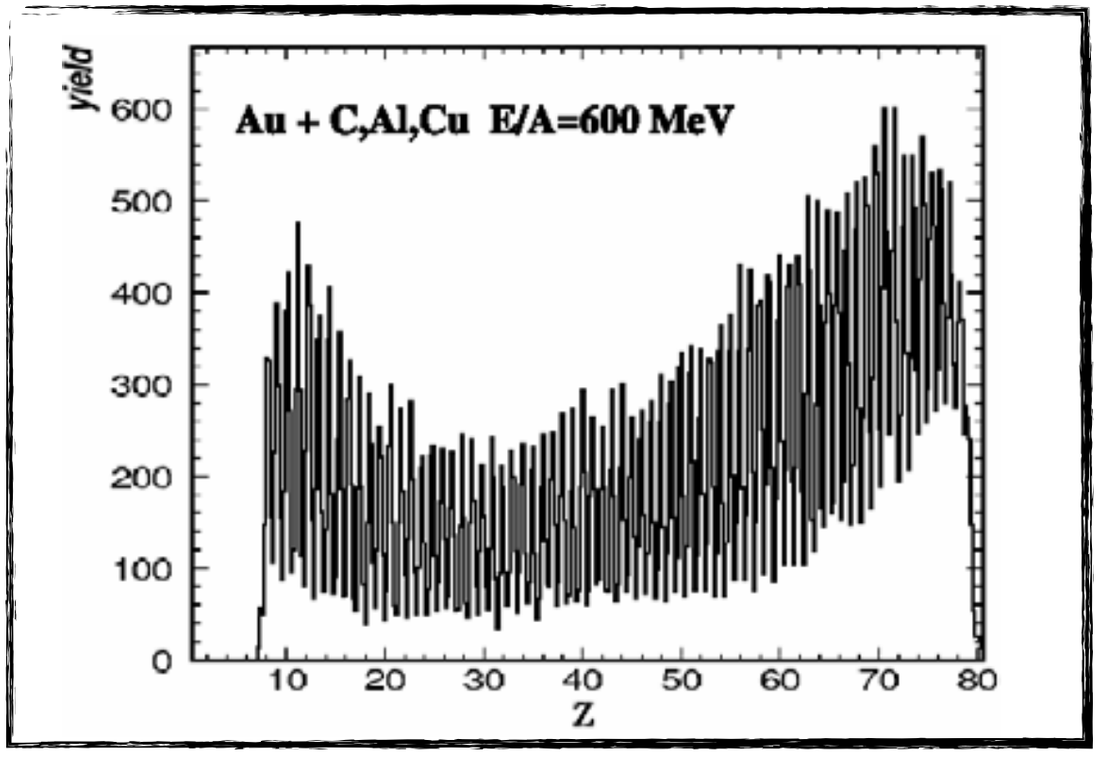

Multiple sampling ionization chamber

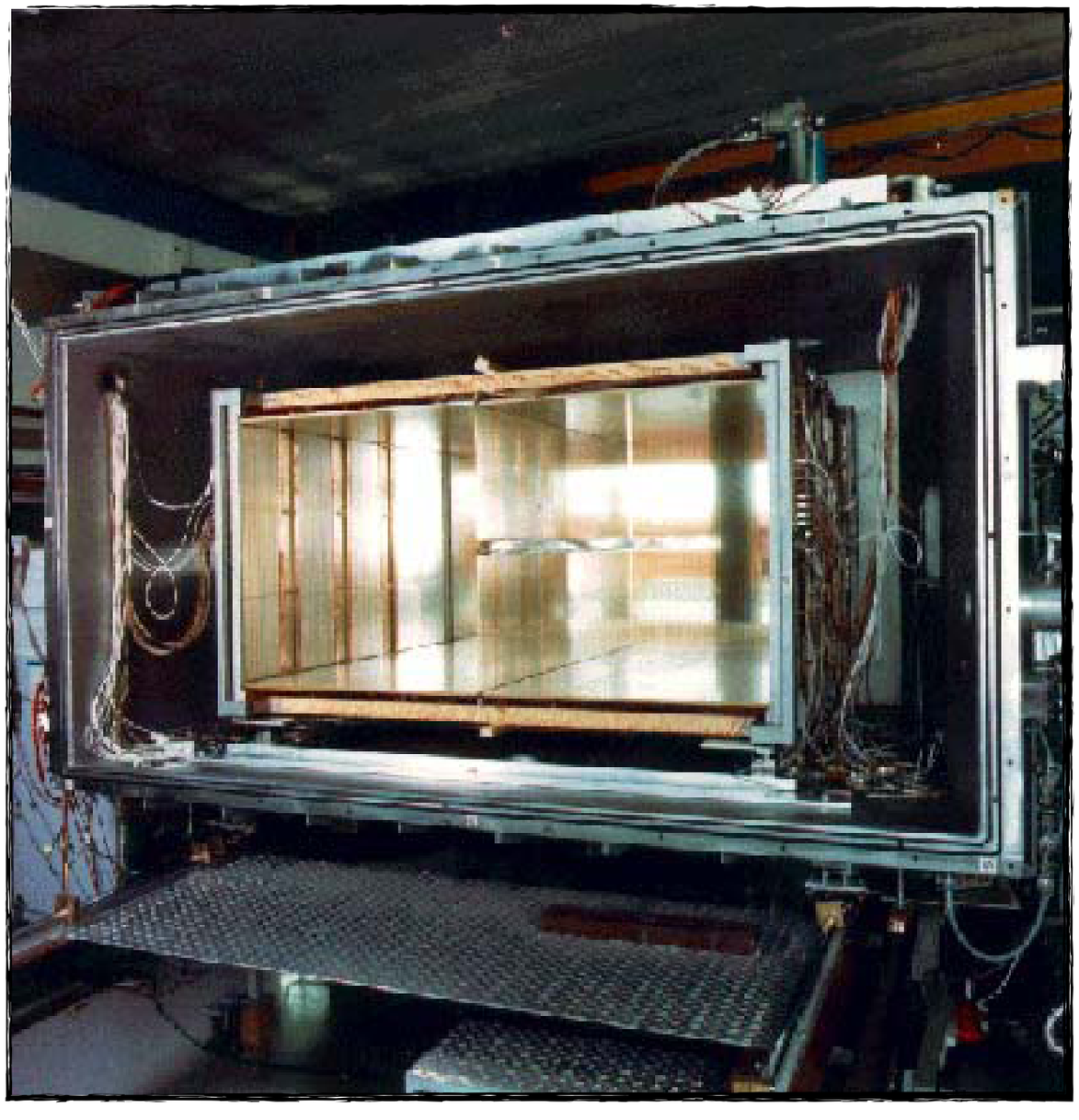

Ionization Chambers – Na 48

Liquid Krypton Ionization Chamber

Homogeneous LKr; gain = 1
184 cells formed by thin electrodes; cell size: 2x2 cm^2
Each cell formed by two drift gaps sharing readout electrode
Electrodes: CuBe ribbons

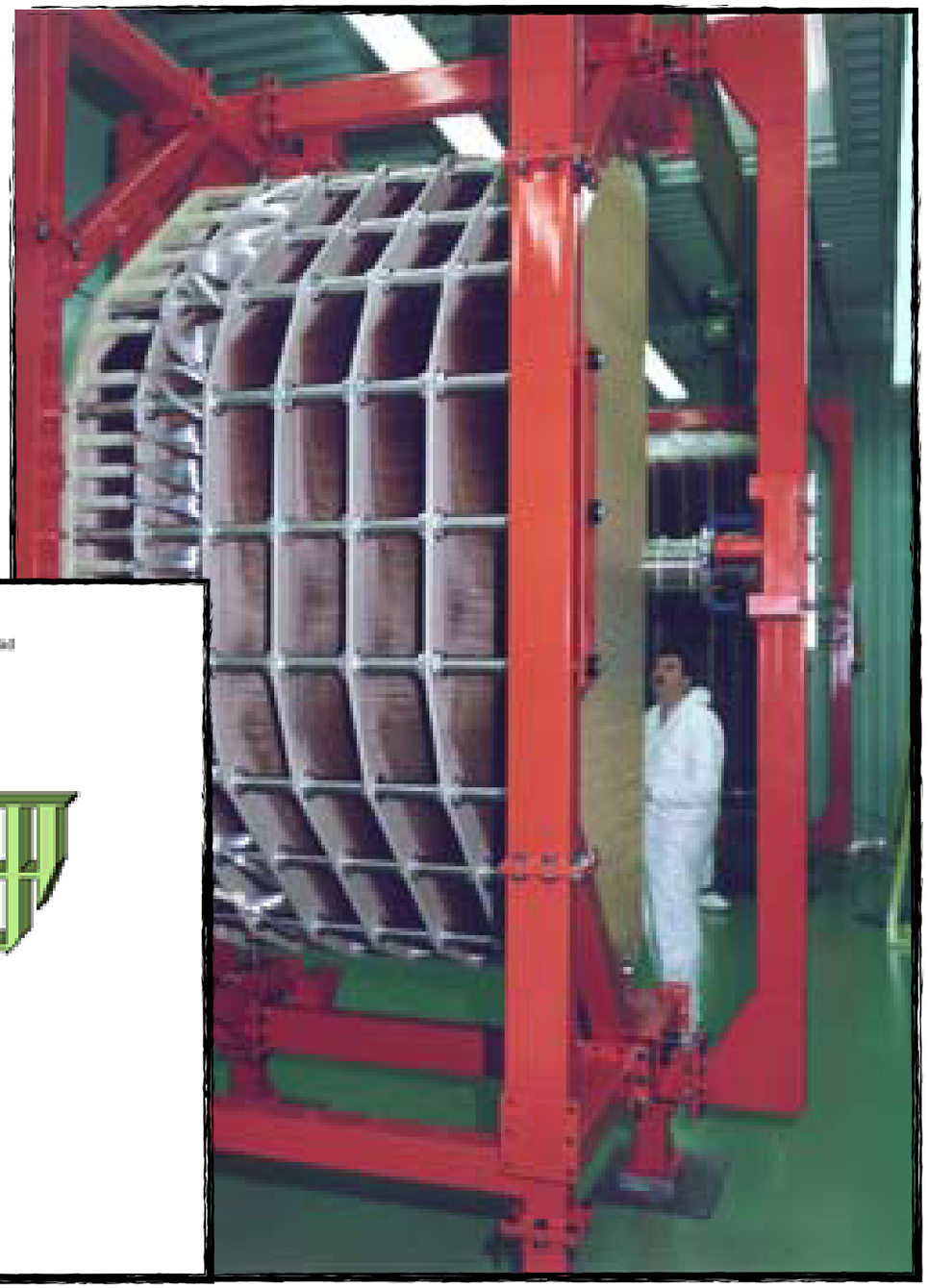

LKr Calorimeter Electrode Structure

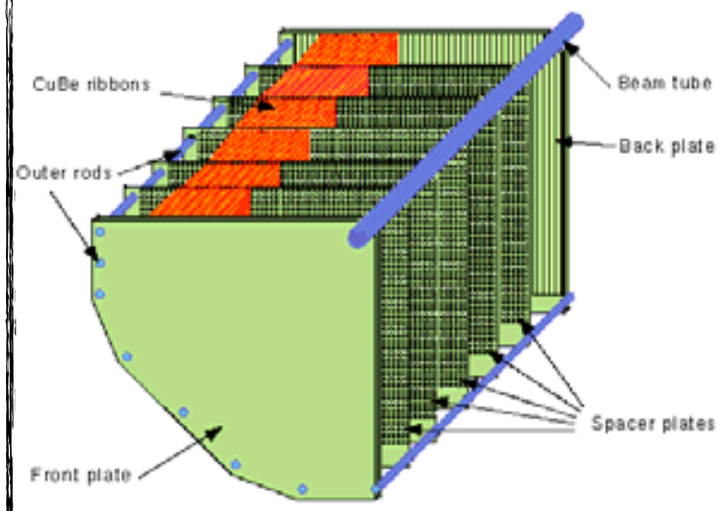

Detail on ribbons and spacer-plate

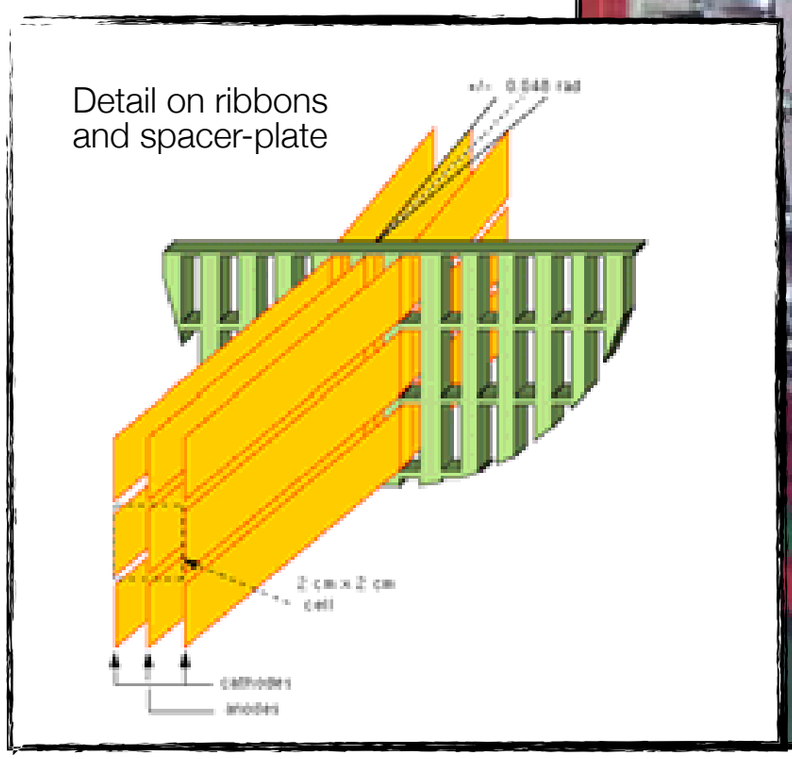

Drift Chambers – Principle

Measure drift time t_D
[need to know t_0; fast scintillator, beam timing]

Determine location of original ionization:

$$x = x_0 \pm v_D \cdot t_D$$
$$y = y_0 \pm v_D \cdot t_D$$

If drift velocity changes along path:

$$x = \int_0^{t_D} v_D \, dt$$

In any case:
Need well-defined drift field ...

Simple Drift Chamber Setup

But: here, uniform drift field requires high-voltages in case of large area detectors

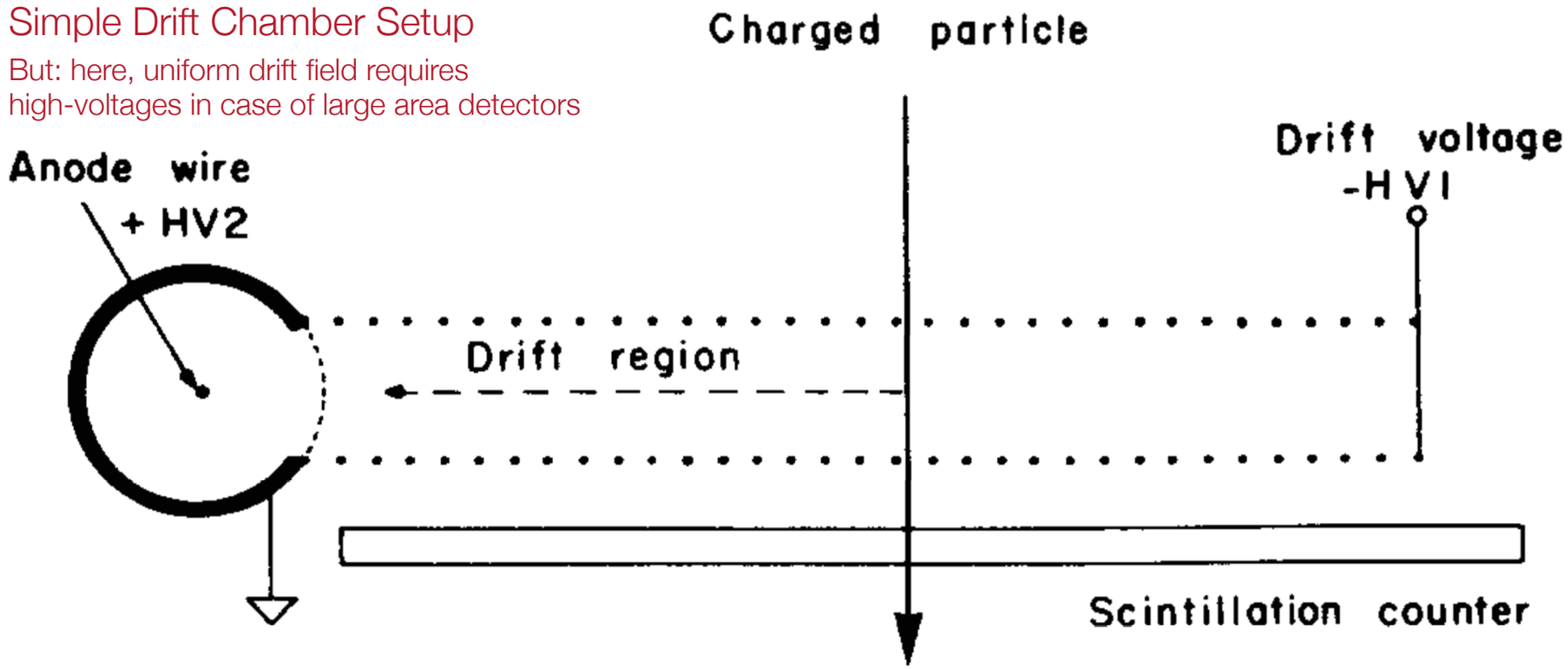

Drift Chambers – The First One

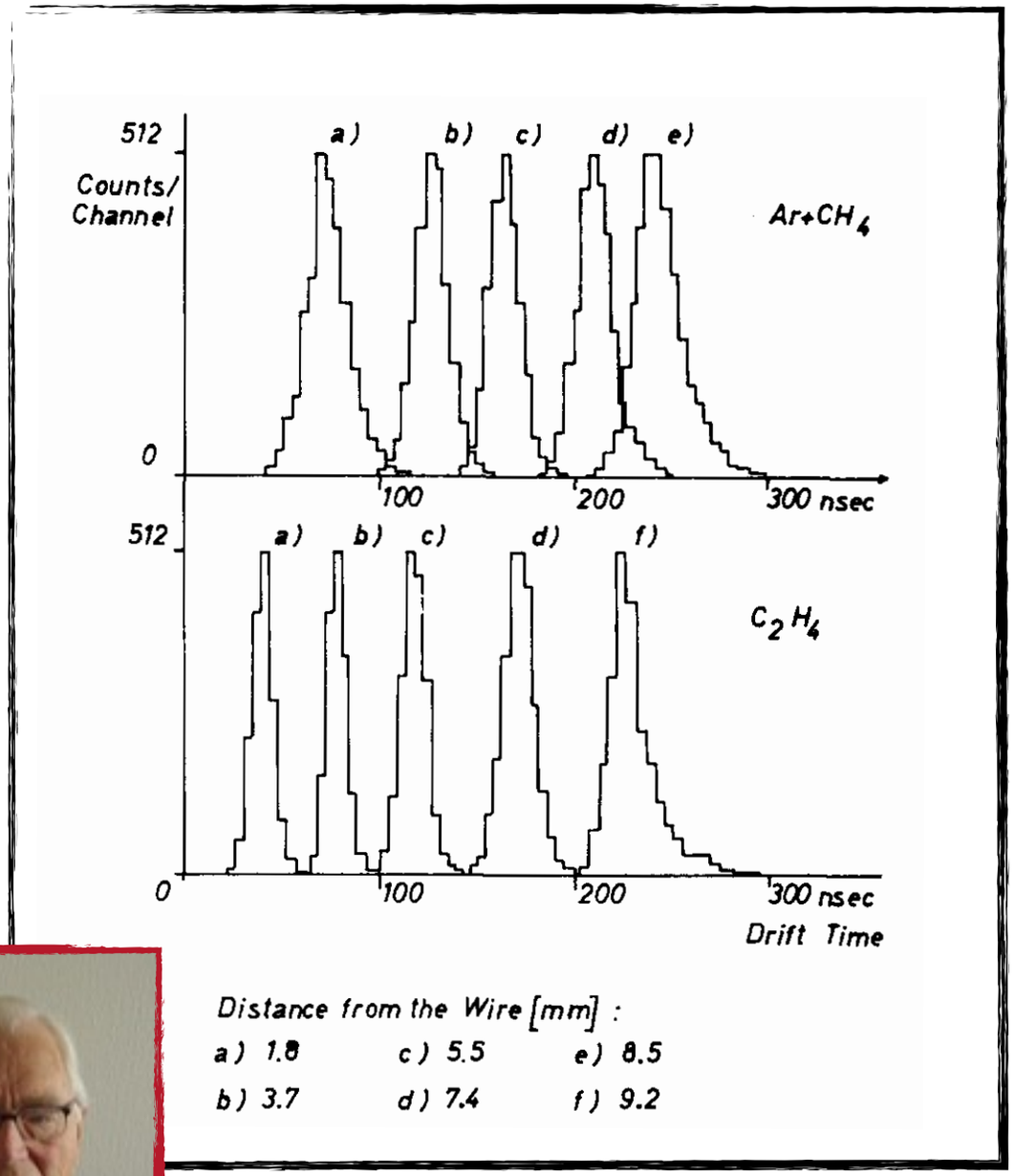

Drift Time Distribution
in Ar+CH_4 and C_2H_4

J.Heintze

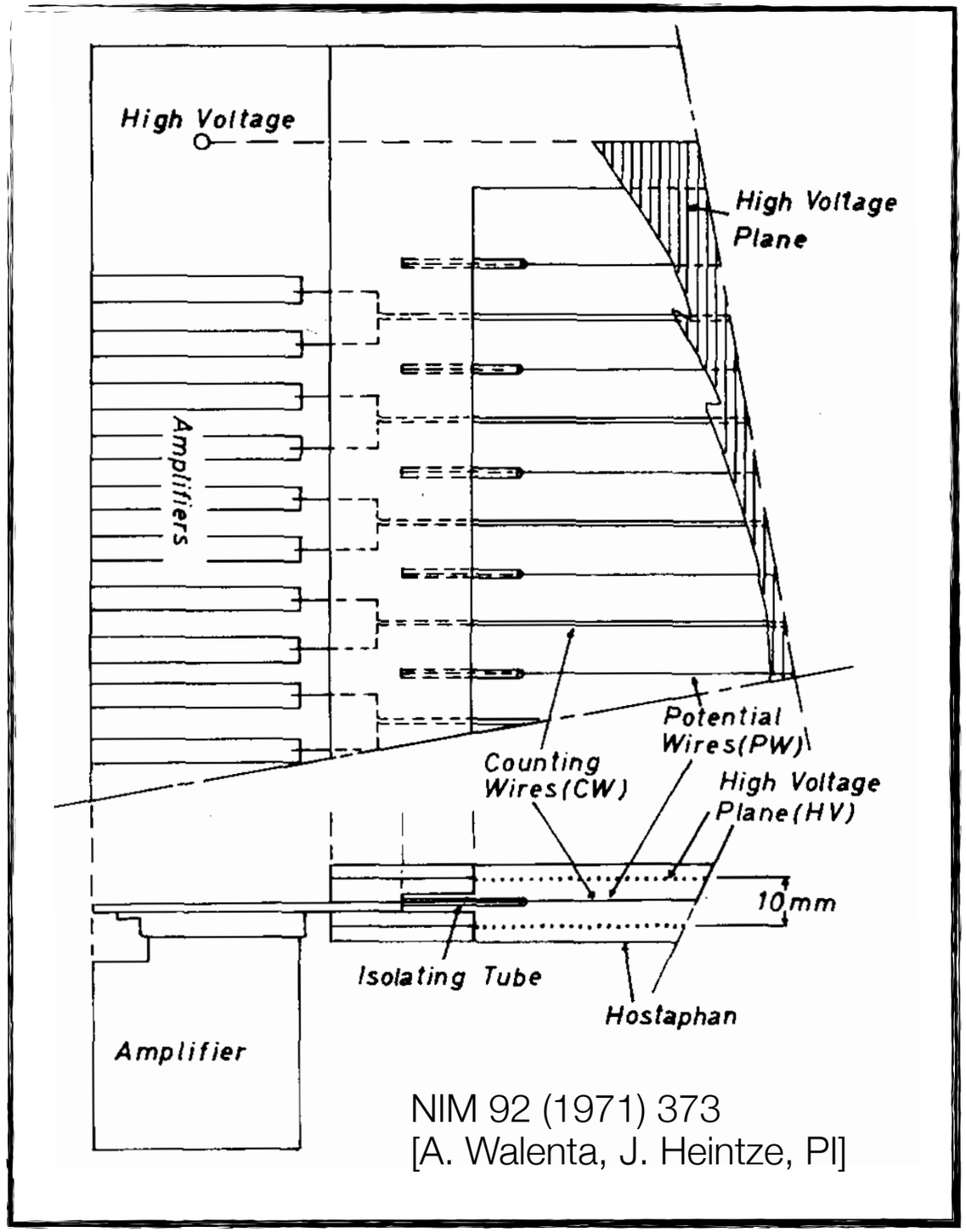

NIM 92 (1971) 373
[A. Walenta, J. Heintze, Pl]

Drift Chambers – Field Formation

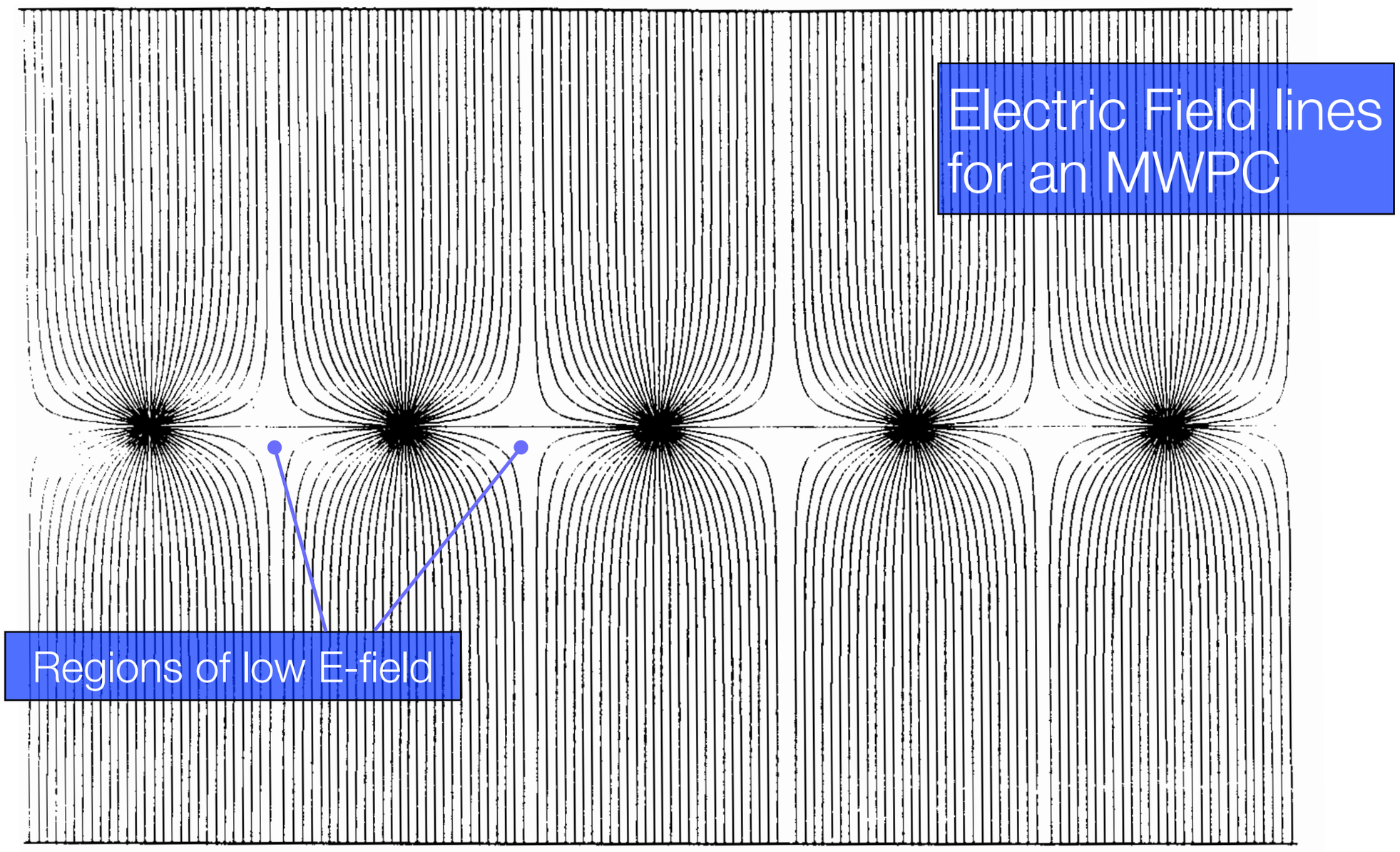

Drift Chambers – Field Formation

Modified MWPC ...

Introduce field wires to avoid
low field regions, i.e. long drift-times

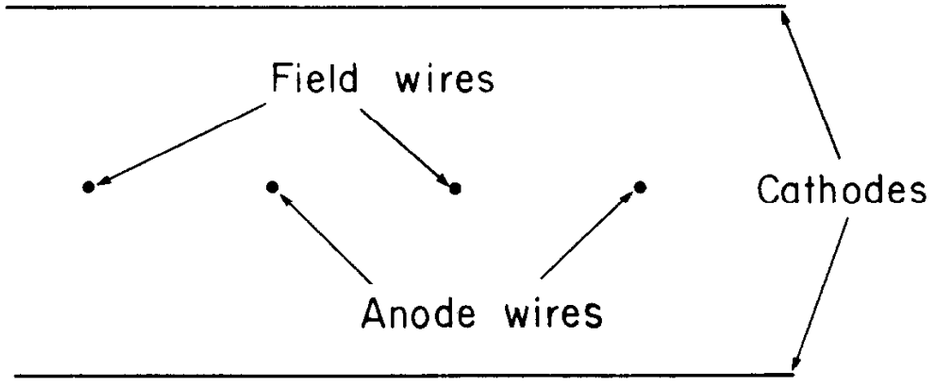

Field wires are
at negative potential ...

Anode wires are
at positive potential ...

Cathode planes are
at zero potential ...

But:

Uniform drift field requires:
Gap length/wire spacing ≈ 1

i.e. for typical convenient wire spacing
one needs thick chambers ...

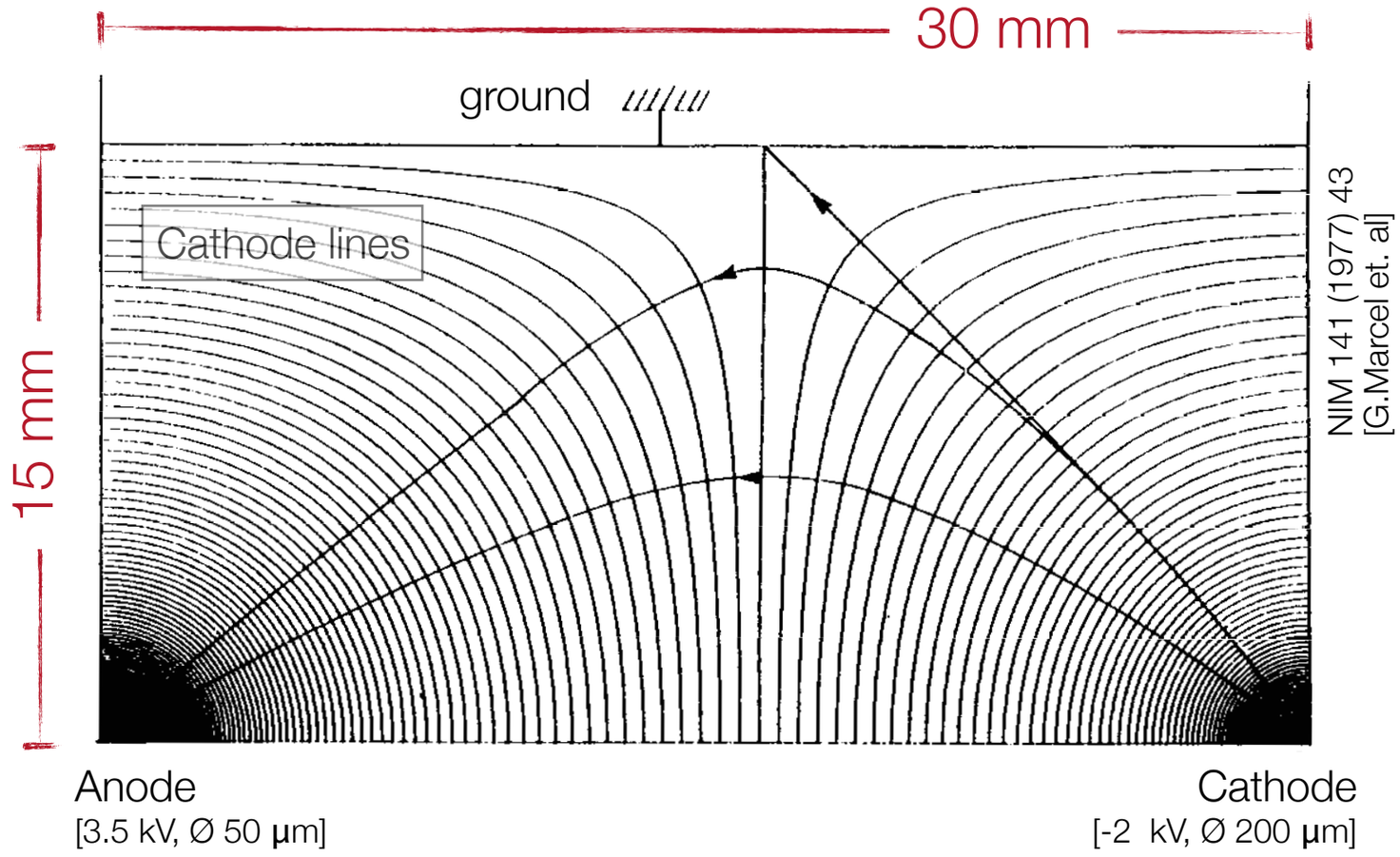

Drift Chambers – Field Formation

Principle of an
adjustable field multi-wire drift chamber

Introduction of voltage divider
via cathode wire planes ...

Features:

very few (or only one) anode wires
space point resolution limited by mechanical accuracy
[for large chambers: $\sigma \approx 200\ \mu m$]

But: hit density needs to be low.

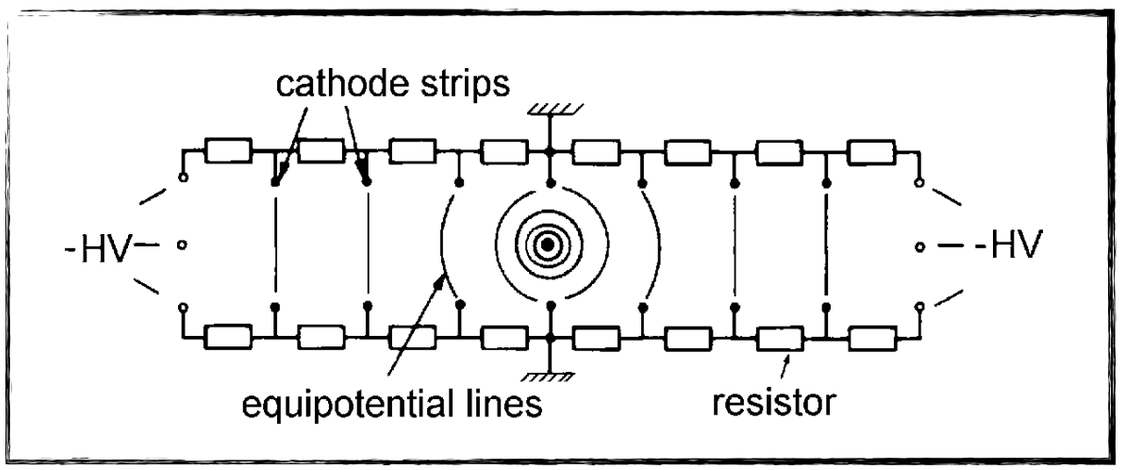

Schematics of voltage divider chain

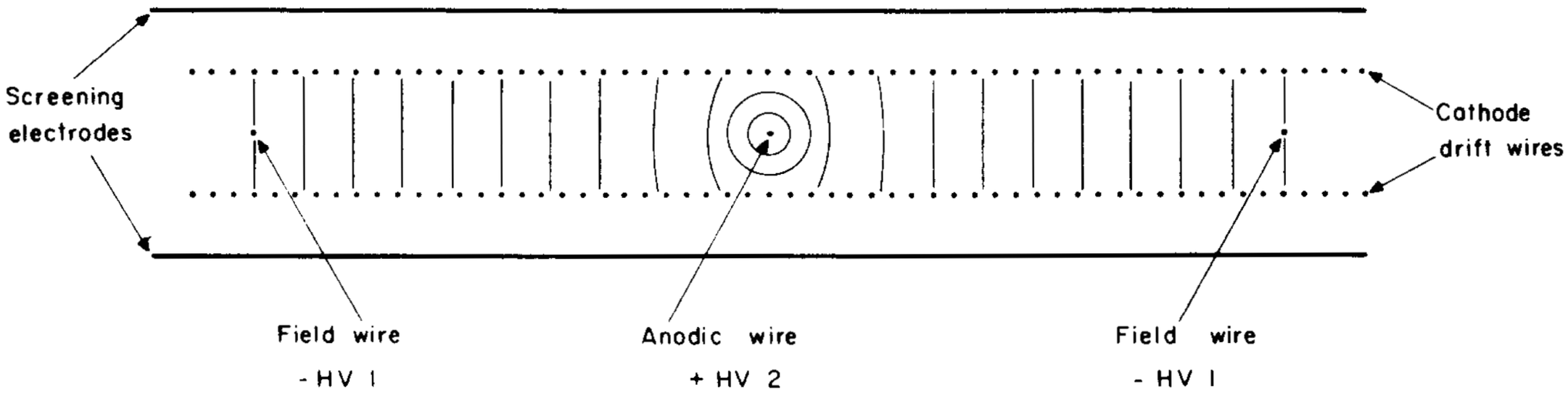

Drift Chambers – Field Formation

Drift time space relation

for a large drift chamber (80x80 cm^2) with only one anode wire

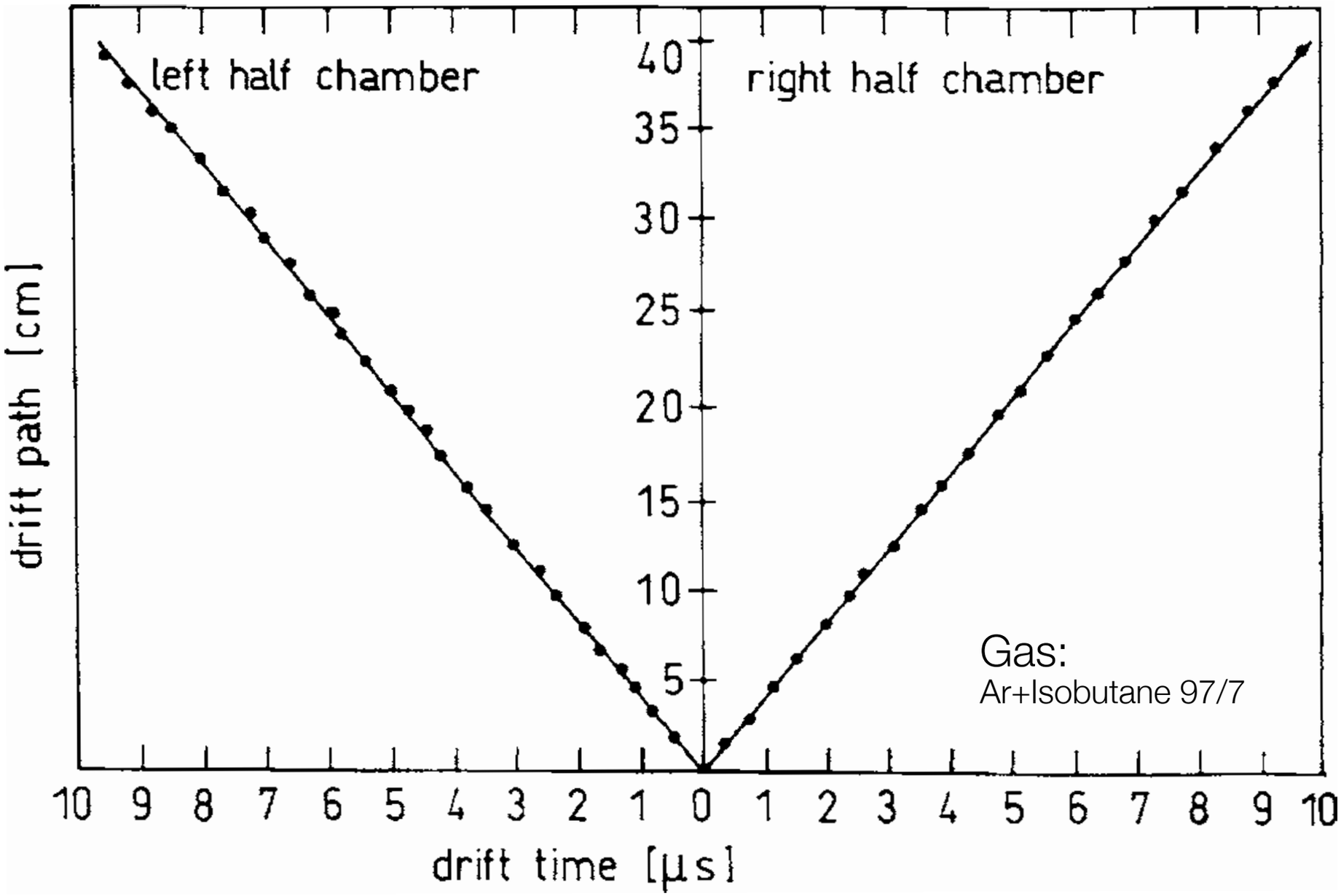

Drift Chambers – Field Formation

Alternative:

Field formation by charging
(insulated) chamber walls with ions ...

Electrodeless drift chamber
[Allison et al., 1982]

Requires some charging time ...

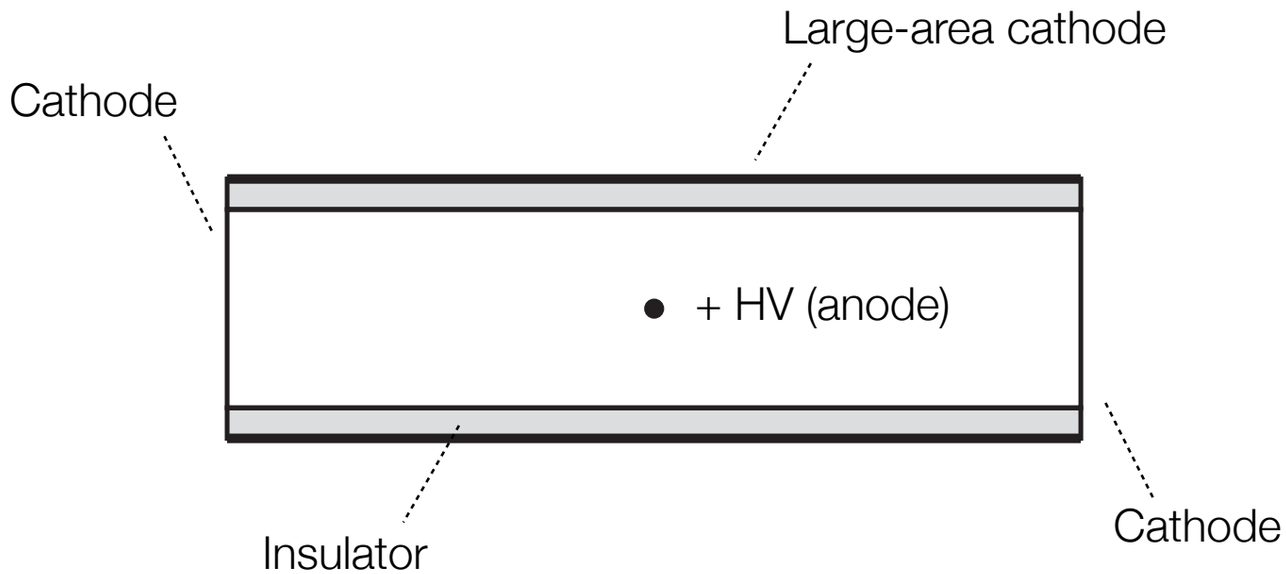

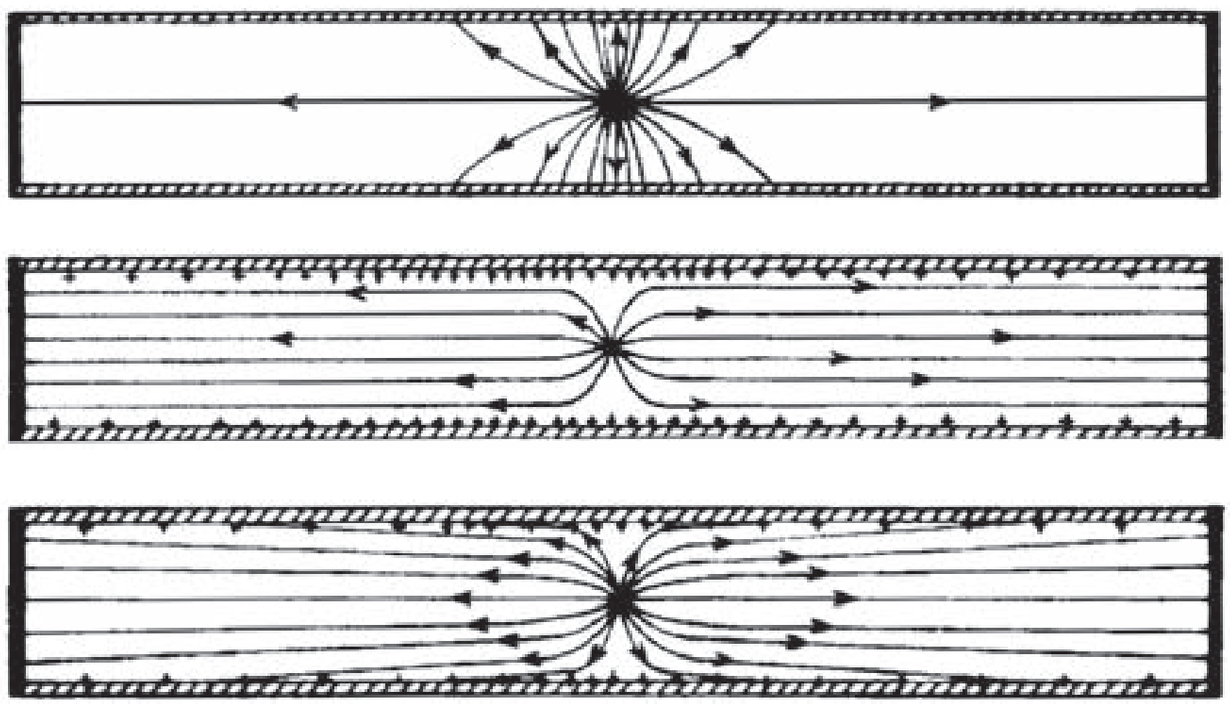

Before charging up:
field line end at cathode ...

After charging time:
no field line end at cathode ...

To avoid overcharging:
Finite resistance of insulator
[i.e. some field lines end at cathode]

Cylindrical Drift Chambers

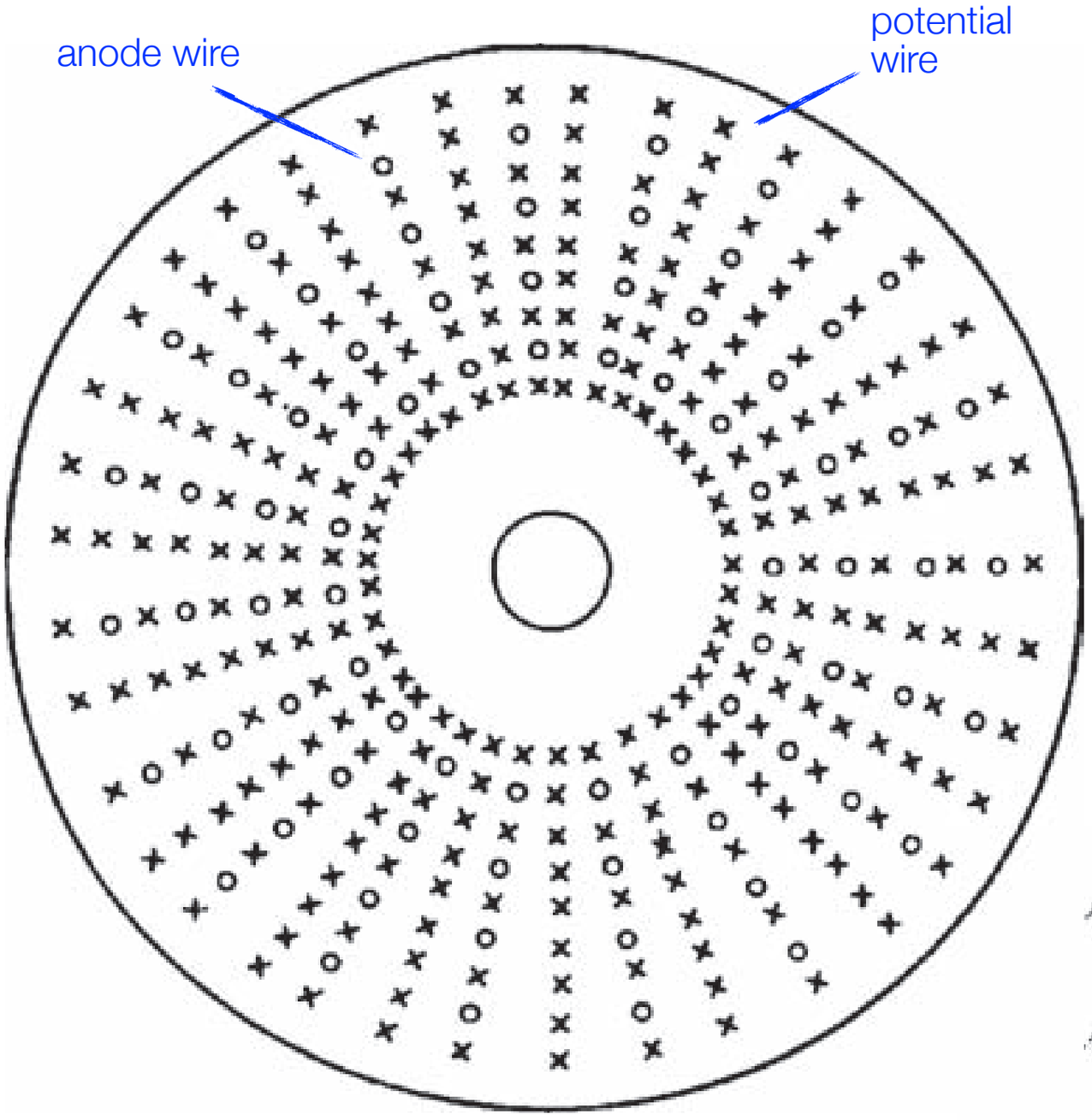

Application:

Collider experiments
[cylindrical wire arrangement needed]

Characteristica:

Cylindrical symmetry
Open drift cell geometry

Require: Simple space-time relation
given by E,B field and drift cell geometry

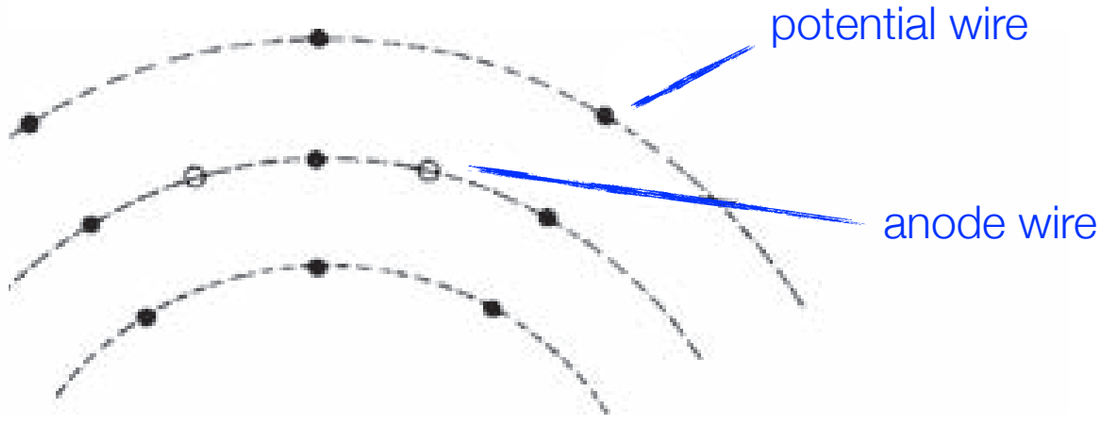

Cylindrical Drift Chambers

A Open
drift-cells geometry

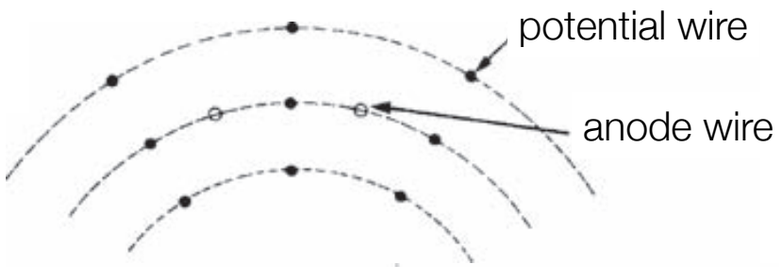

B

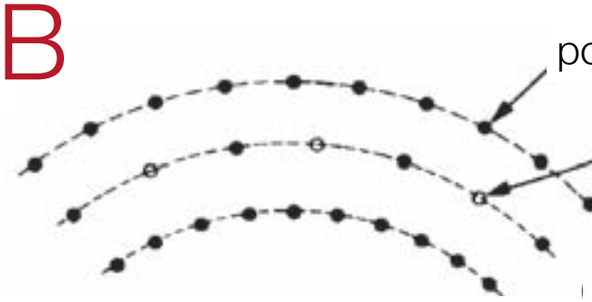

B Closed
drift-cells geometry
[more wires]

C Hexagonal
drift-cells geometry
[intermediate configuration]

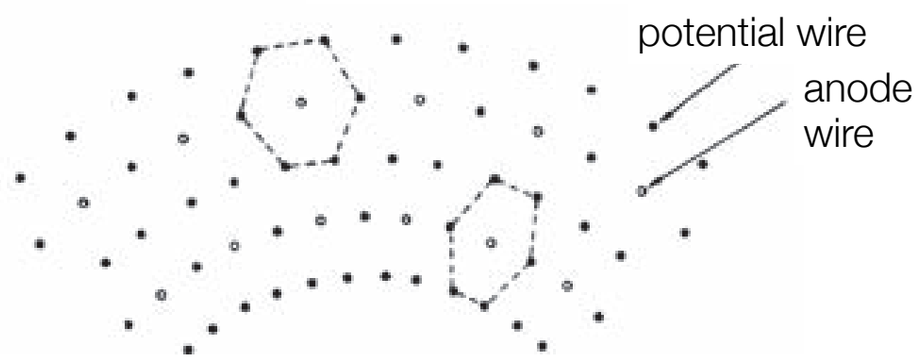

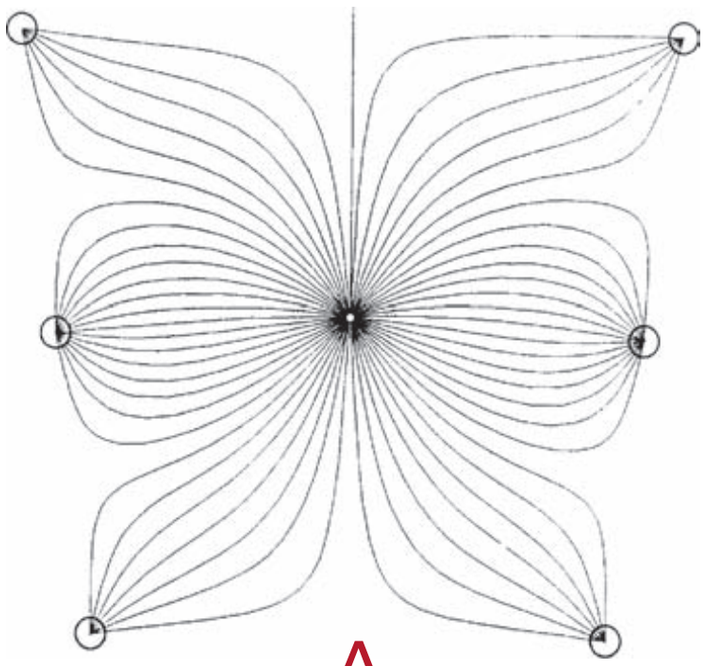

A

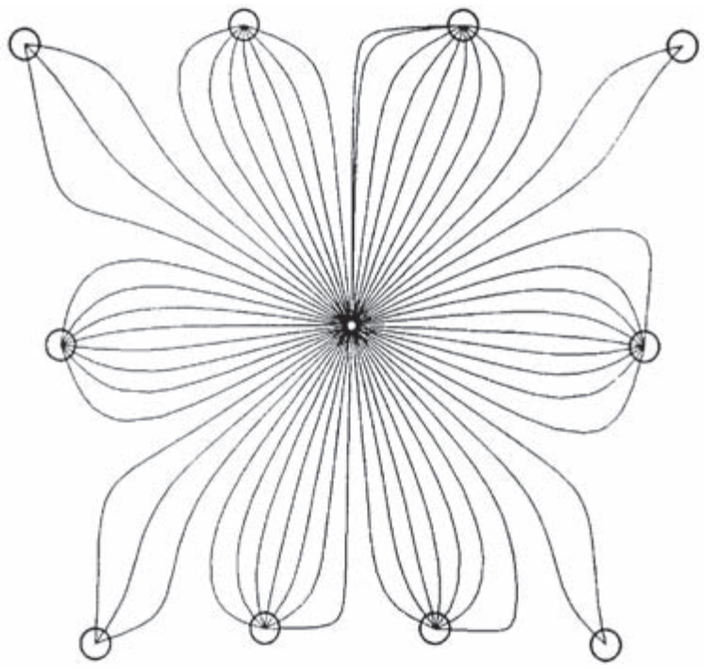

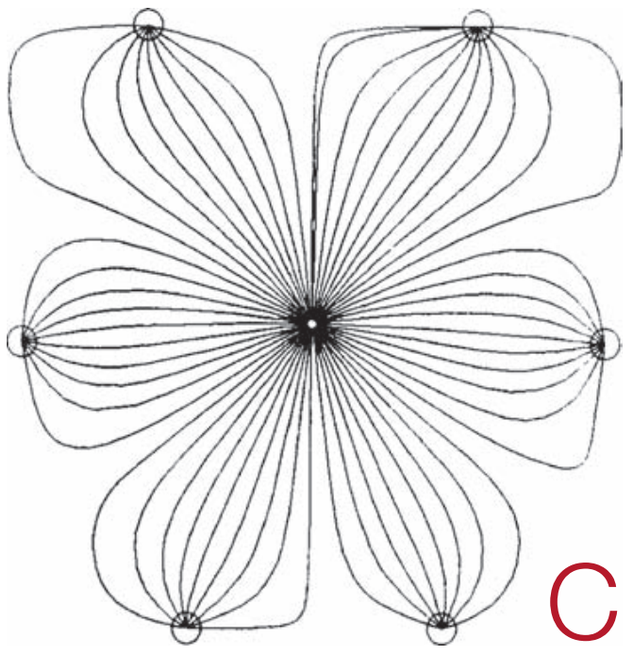

C

Drift Chambers – Lorentz Angle

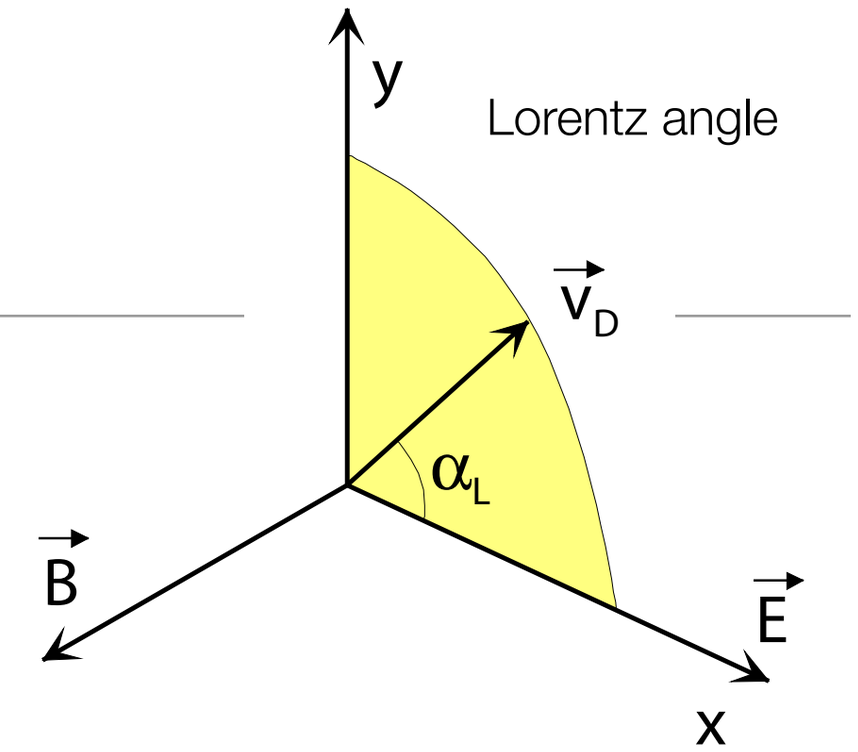

Require B field for momentum measurement ...

In general drift field E ⊥ to B field ...

➛ Lorentz angle: $\alpha_L = \sphericalangle(\vec{v}_D, \vec{E})$ ...

Reminder:

$$\vec{v}_D = \frac{\mu|\vec{E}|}{1+\omega^2\tau^2}\left[\hat{\vec{E}} + \overbrace{\omega\tau\hat{\vec{E}}\times\hat{\vec{B}}}^{\perp \text{ to E,B}} + \overbrace{\omega^2\tau^2(\hat{\vec{E}}\cdot\hat{\vec{B}})\hat{\vec{B}}}^{\text{in direction of B}}\right]$$

Using:

$$v_{D,x} = \frac{\mu E}{1+\omega^2\tau^2}$$

$$v_{D,y} = \frac{\mu E}{1+\omega^2\tau^2}\cdot\omega\tau$$

➛ $$\tan\alpha_L = \omega\tau = v_D\frac{B}{E}$$

[with $\omega = \frac{eB}{m}$ and $\tau = \frac{mv_D}{eE}$]

without B field

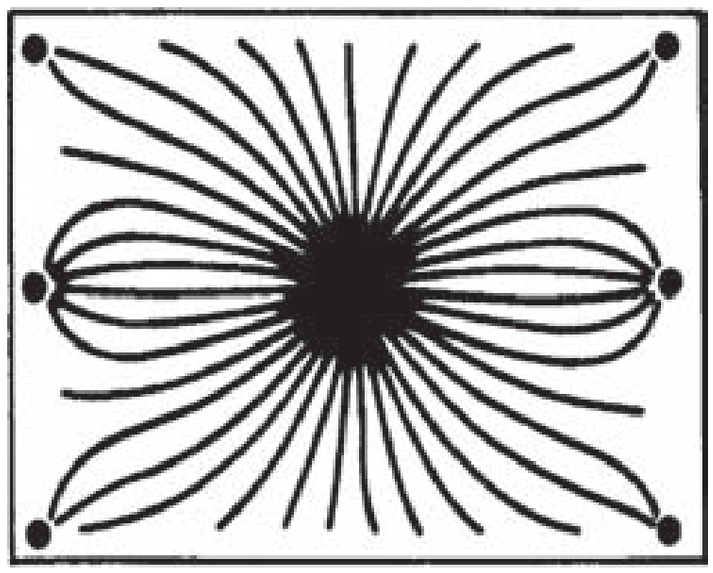

with B field

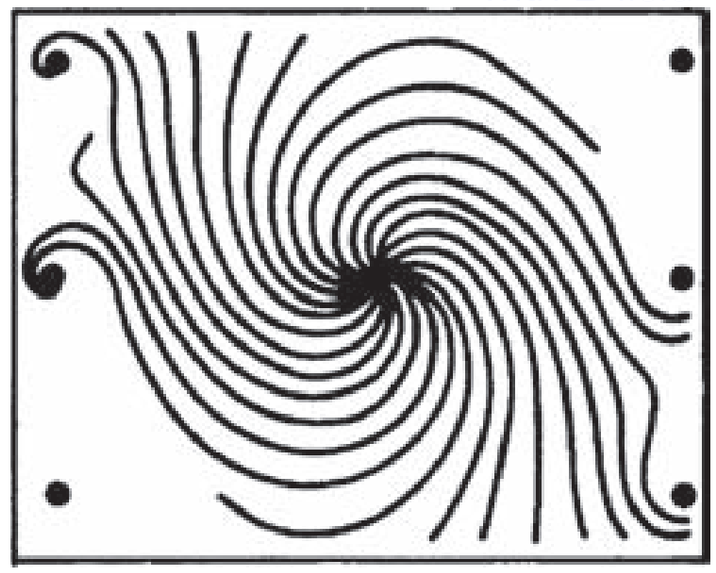

Drift Chamber – Spatial Resolution

Resolution determined by
accuracy of drift time measurement ...

Influenced by:

Diffusion [$\sigma_{Diff.} \sim \sqrt{x}$]

see above: $\sigma^2 \sim 2Dt = 2Dx/v_D \sim x$ ...

δ-electrons [σ_δ = const.]

independent of drift length; yields constant
term in spatial resolution ...

Electronics [$\sigma_{electronics}$ = const.]

contribution also independent of drift length ...

Primary ionization statistics [$\sigma_{prim} = 1/x$]

Spatial fluctuations of charge-carrier production result in
large drift-path differences for particle trajectories close to the anode ...
[minor influence for tracks far away from anode]

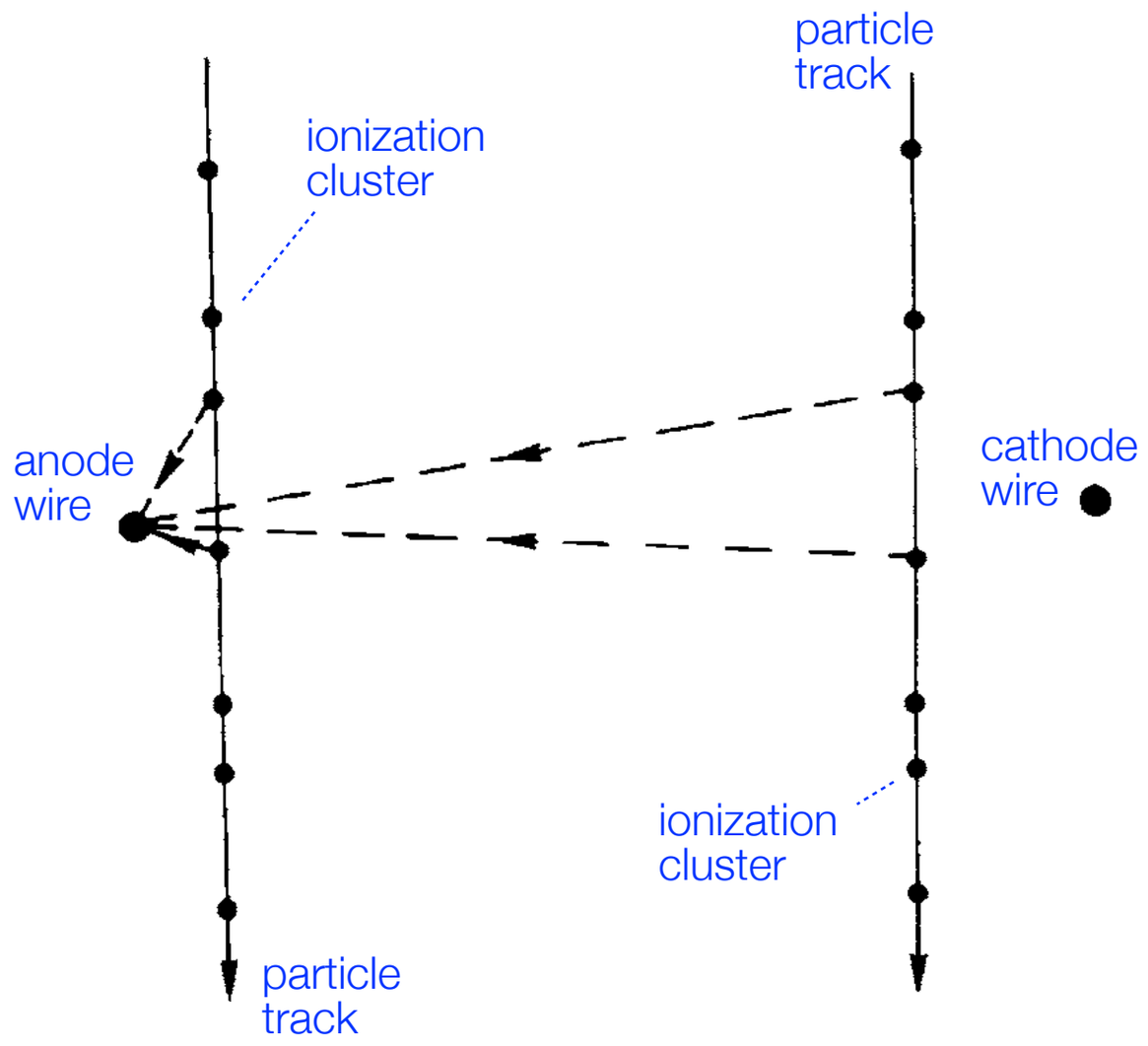

Drift Chamber – Spatial Resolution

Primary ionization statistics:

Step 1: Consider a track passing through an anode wire ...

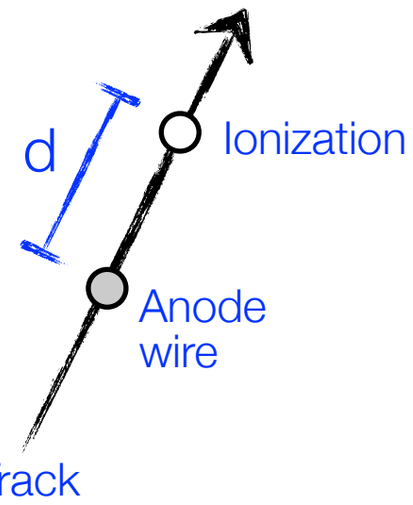

Probability of no ionization within distance d:

$$P_0(d) = e^{-2Nd}$$

with

N: number of ionizations per unit length

Average minimum distance of closest ionization cluster:

Normalization

$$\delta x_0 = \langle d_{\min} \rangle = \int_0^\infty x e^{-2Nx}\, 2N\, dx = \frac{1}{2N}$$

$$\sigma^2_{\langle d_{\min} \rangle} = \int_0^\infty (x - \frac{1}{2N})^2 e^{-2Nx}\, 2N\, dx = \frac{1}{4N^2}$$

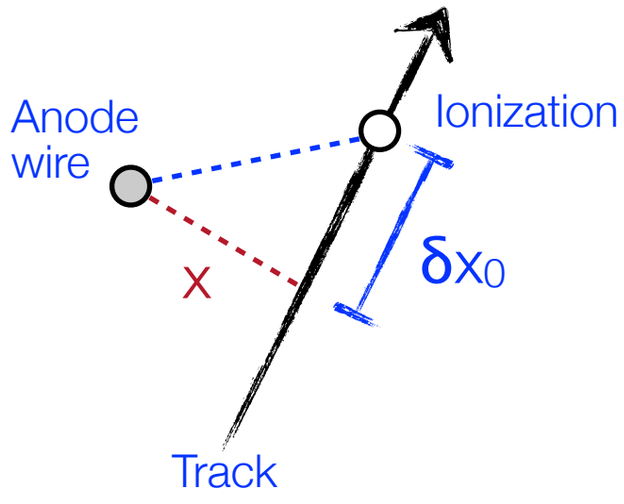

Step 2: Track at distance x ...

$$\delta x = \sqrt{x^2 + (\delta x_0)^2} - x = x\left(\sqrt{1 + \left(\frac{\delta x_0}{x}\right)^2} - 1\right) \approx \frac{x}{2}\left(\frac{\delta x_0}{x}\right)^2 \propto \frac{1}{x}$$

Drift Chamber – Spatial Resolution

$$\sigma_x^2 = \underbrace{\left(\frac{1}{64N^2}\right)\cdot\frac{1}{x^2}}_{1^{st}\text{ ionization statistics}} + \underbrace{\frac{2D}{v_d}\cdot x}_{\text{diffusion}} + \underbrace{\sigma^2_{\text{const}}}_{\substack{\text{electronics}\\ \delta\text{-electrons}}}$$

Possible improvements:

Increase N by increasing pressure ...

Decrease D by increasing pressure ...

$$D \sim \frac{\lambda_0^2}{\tau} \sim \frac{{}^1\!/\!_{n^2}}{{}^1\!/\!_n} \sim \frac{1}{n}$$

[n: particle density in gas]
[increases with pressure]

i.e.: increase pressure ...
[up to 4 atm possible]

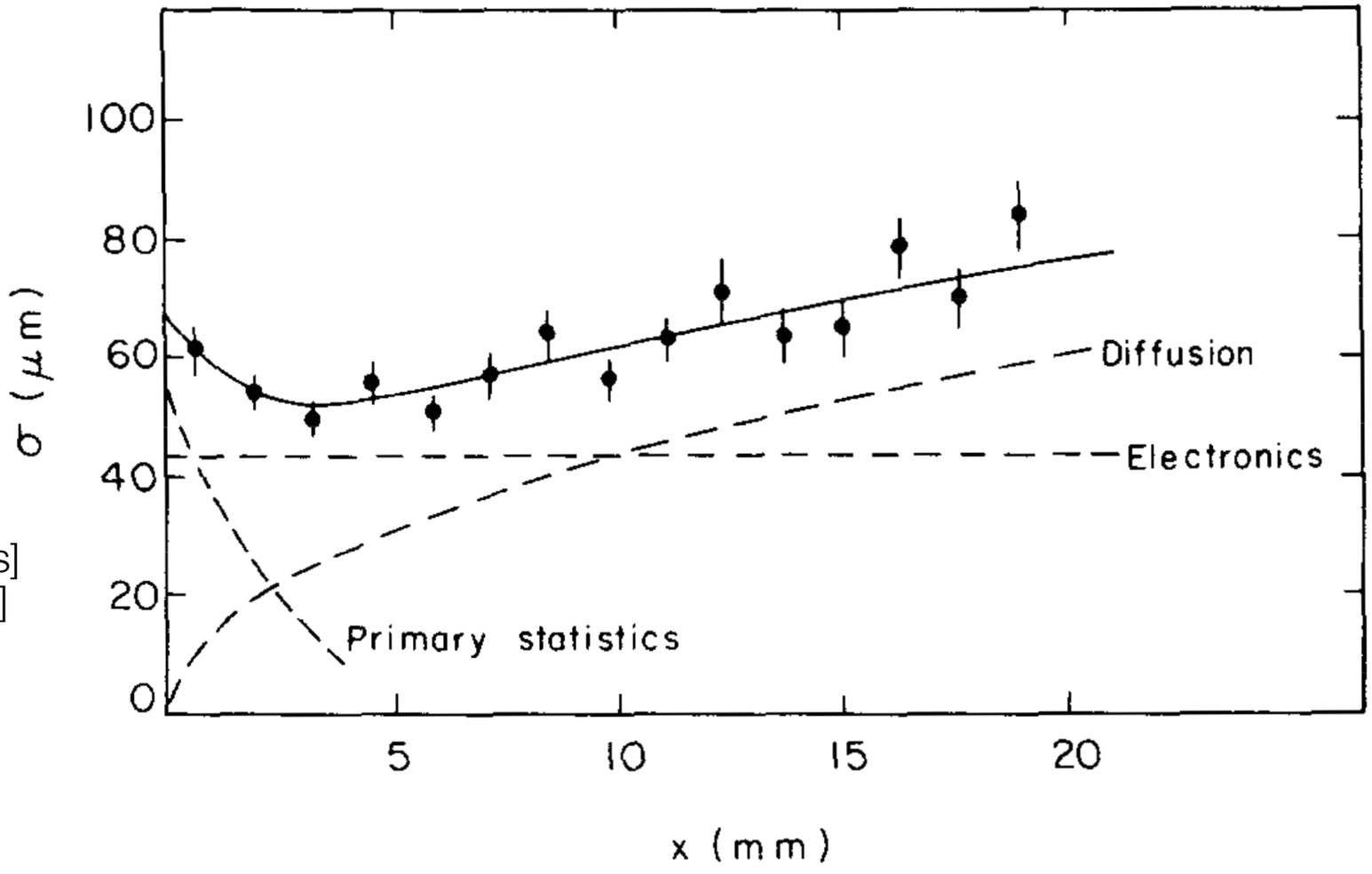

Drift Chamber – Determination of z

Principle of
Charge Devision Method

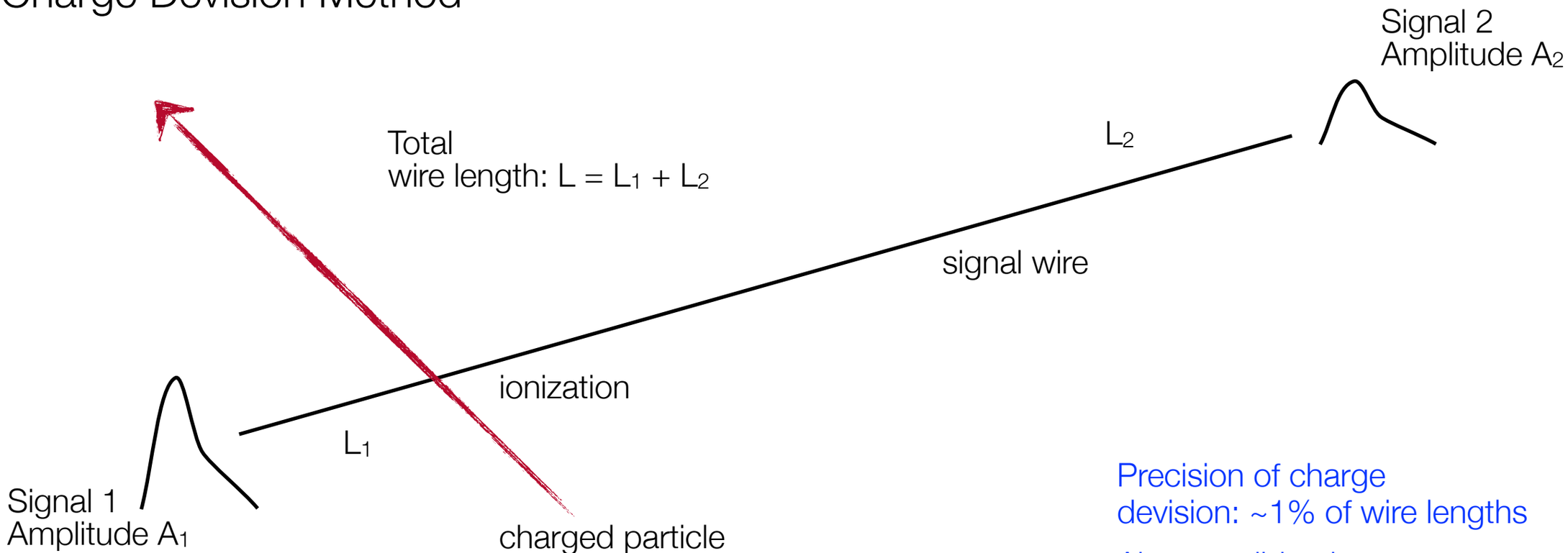

Precision of charge devision: ~1% of wire lengths

Also possible: time measurement on both ends

Determination of L_1, L_2:

$$L_2 = \frac{A_1}{A_1 + A_2} \cdot L \qquad L_1 = \frac{A_2}{A_1 + A_2} \cdot L$$

Magnetic Spectrometer Resolution

Momentum determination
in a cylindrical drift chamber ...

$$\frac{mv^2}{R} = evB \quad \rightarrow \quad p = eB \cdot R$$

$$p\left[\frac{\mathrm{GeV}}{c}\right] = 0.3B\,[\mathrm{m}] \cdot R\,[\mathrm{T}]$$

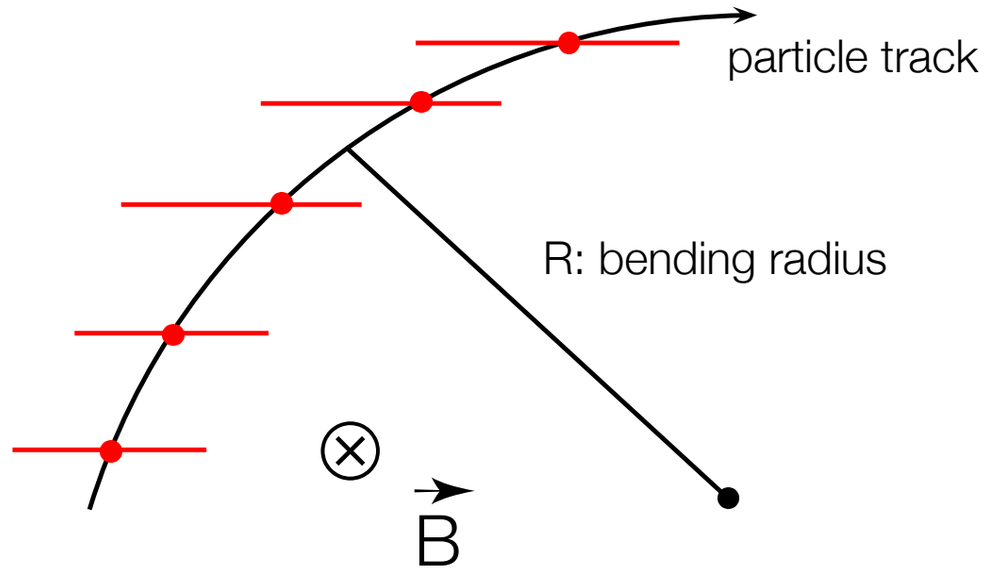

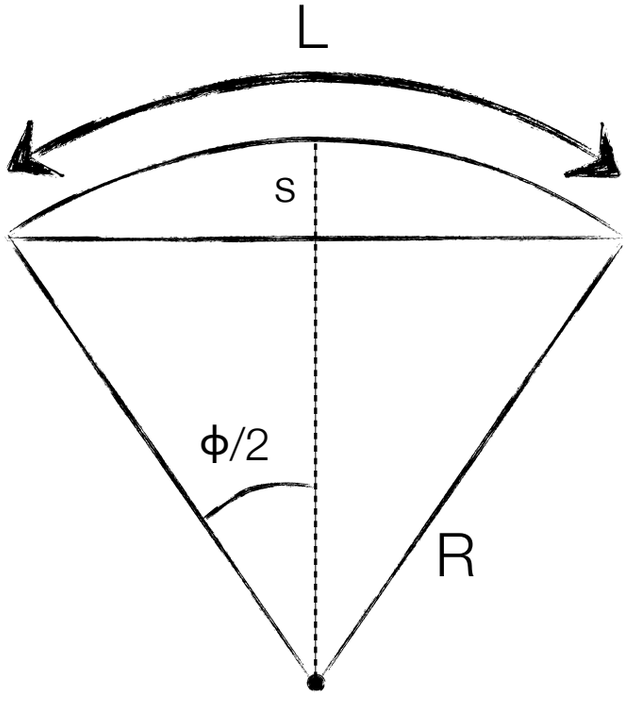

For Sagitta s:

$$s = R - R\cos\frac{\phi}{2} \approx R\,\frac{\phi^2}{8} \qquad \text{with } \phi = \frac{L}{R}$$

$$s = R\frac{L^2}{8R^2} = \frac{L^2}{8R} \quad \text{and} \quad R = \frac{L^2}{8s}$$

$$\rightarrow \quad \frac{\Delta p}{p} = \frac{\Delta R}{R} = \frac{L^2}{8Rs} \cdot \frac{\Delta s}{s}$$

Magnetic Spectrometer Resolution

Momentum measurement uncertainty:

$$\frac{\sigma_p}{p} = \frac{L^2}{8Rs} \cdot \frac{\sigma_s}{s} = \frac{L^2}{8R} \cdot \frac{\sigma_s}{L^4/64R^2} = \frac{\sigma_s}{L^2} \cdot 8R = \frac{\sigma_s}{L^2} \cdot \frac{8p}{eB} \sim p \cdot \frac{\sigma_s}{BL^2}$$

Uncertainty σ_s depends on number and spacing of track point measurements; for equal spacing and large N:

$$\sigma_s = \frac{\sigma_{r\phi}}{8}\sqrt{\frac{720}{N+5}}$$ see: Glückstern, NIM 24 (1963) 381 or Blum & Rolandi, Particle Detection ...

Good momentum resolution:
- large path length L
- large magnetic field B
- good Sagitta measurement

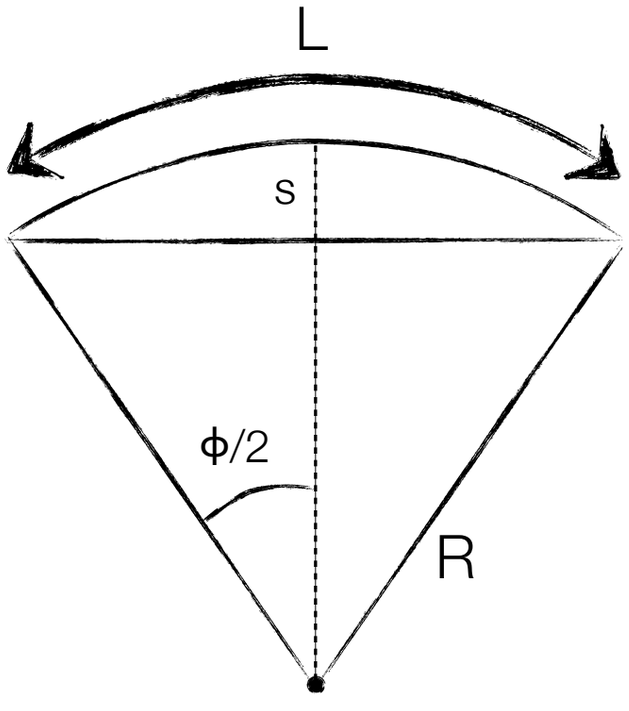

Multiple scattering contribution:

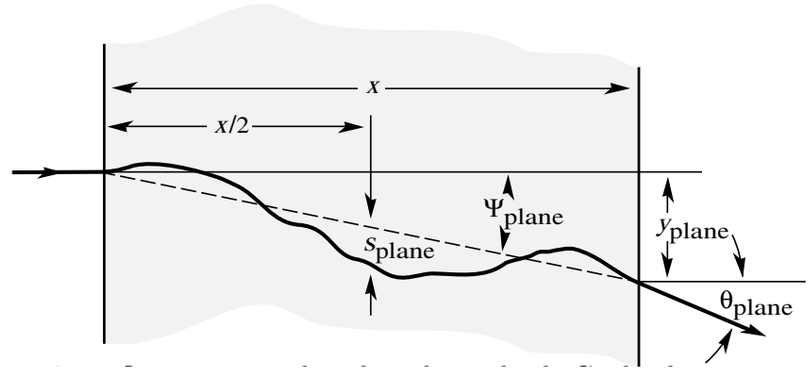

Reminder:

$$\sigma_\phi = \frac{13.6\text{MeV}}{\beta cp} z\sqrt{x/X_0}\,[1 + 0.038\ln(x/X_0)]$$

$$\sigma_\phi \approx \frac{14\ \text{MeV}/c}{p}\sqrt{\frac{L}{X_0}} \quad \text{and} \quad \frac{\sigma_p}{p} = \frac{\sigma_R}{R} = \frac{\sigma_\phi}{\phi}$$

as $R = \frac{L}{\phi}$

Magnetic Spectrometer Resolution

Multiple scattering contribution:
[cont'd]

momentum independent

$$\frac{\sigma_p}{p} = \frac{\sigma_\phi}{\phi} = \frac{14\ \mathrm{MeV}/c}{p}\sqrt{\frac{L}{X_0}} \cdot \frac{R}{L} = \frac{14\ \mathrm{MeV}/c}{p}\sqrt{\frac{1}{LX_0}} \cdot \frac{p}{eB} \sim \frac{1}{\sqrt{LX_0}B}$$

Generally p_t measured:

$$\left(\frac{\sigma_{p_t}}{p_t}\right)^2 = \mathrm{const} \cdot \left(\frac{p_t}{BL^2}\right)^2 + \mathrm{const} \cdot \left(\frac{1}{B\sqrt{LX_0}}\right)^2$$

For momentum p:

$$\left(\frac{\sigma_p}{p}\right)^2 = \left(\frac{\sigma_{p_t}}{p_t}\right)^2 + \left(\frac{\sigma_\theta}{\sin\theta}\right)^2$$

using $p = \frac{p_t}{\tan\theta}$

Examples:

Argus: $\sigma_{pt}/p_t = 0.009^2 + (0.009\ p_t)^2$

ATLAS: $\sigma_{pt}/p_t = 0.001^2 + (0.0005\ p_t)^2$

[ATLAS nominal; TDR]

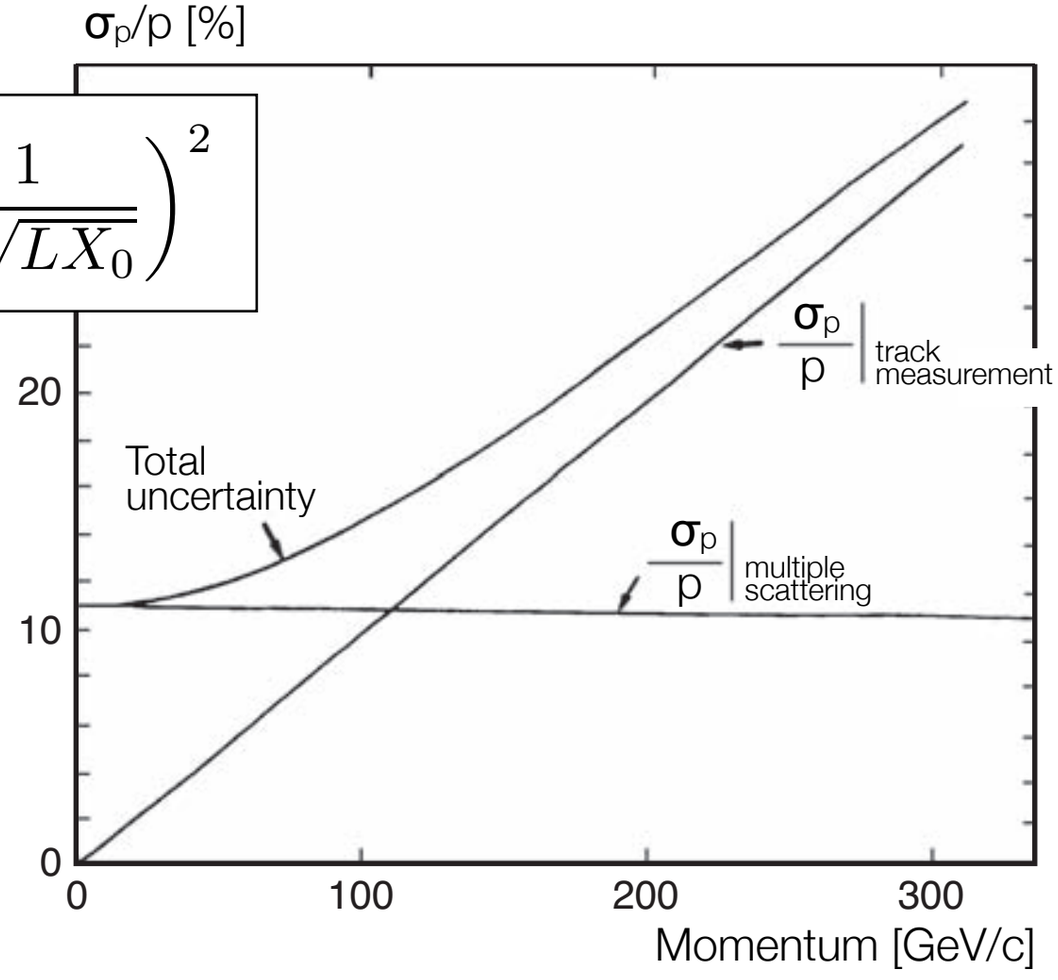

Magnetic Spectrometer Resolution

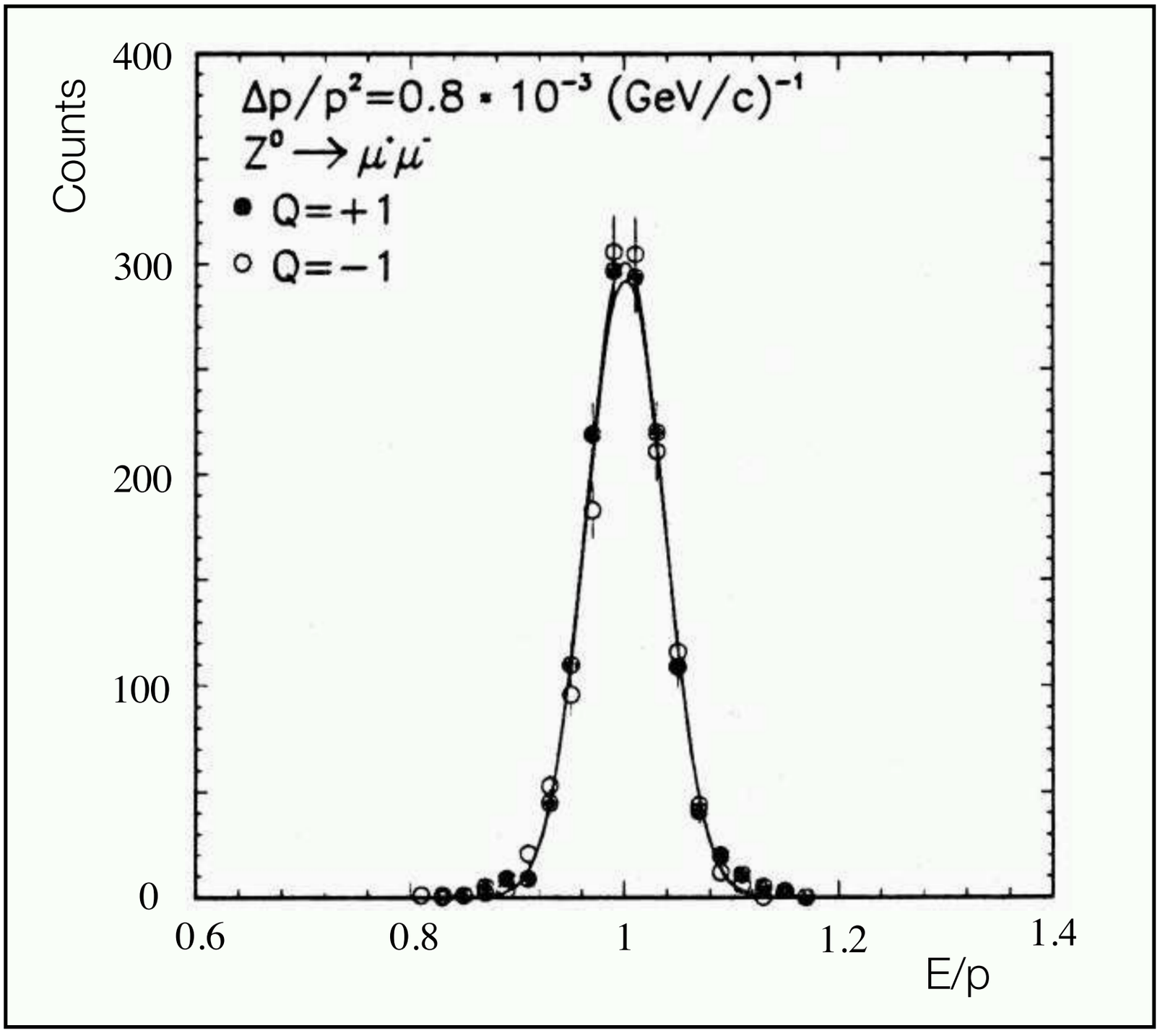

Momentum resolution for muons in Z ➛ μμ

s ~ 1/R ~ 1/p measured!
➛ 1/p is Gaussian

Magnetic Spectrometer Resolution

Momentum determination
in fixed target experiments ...

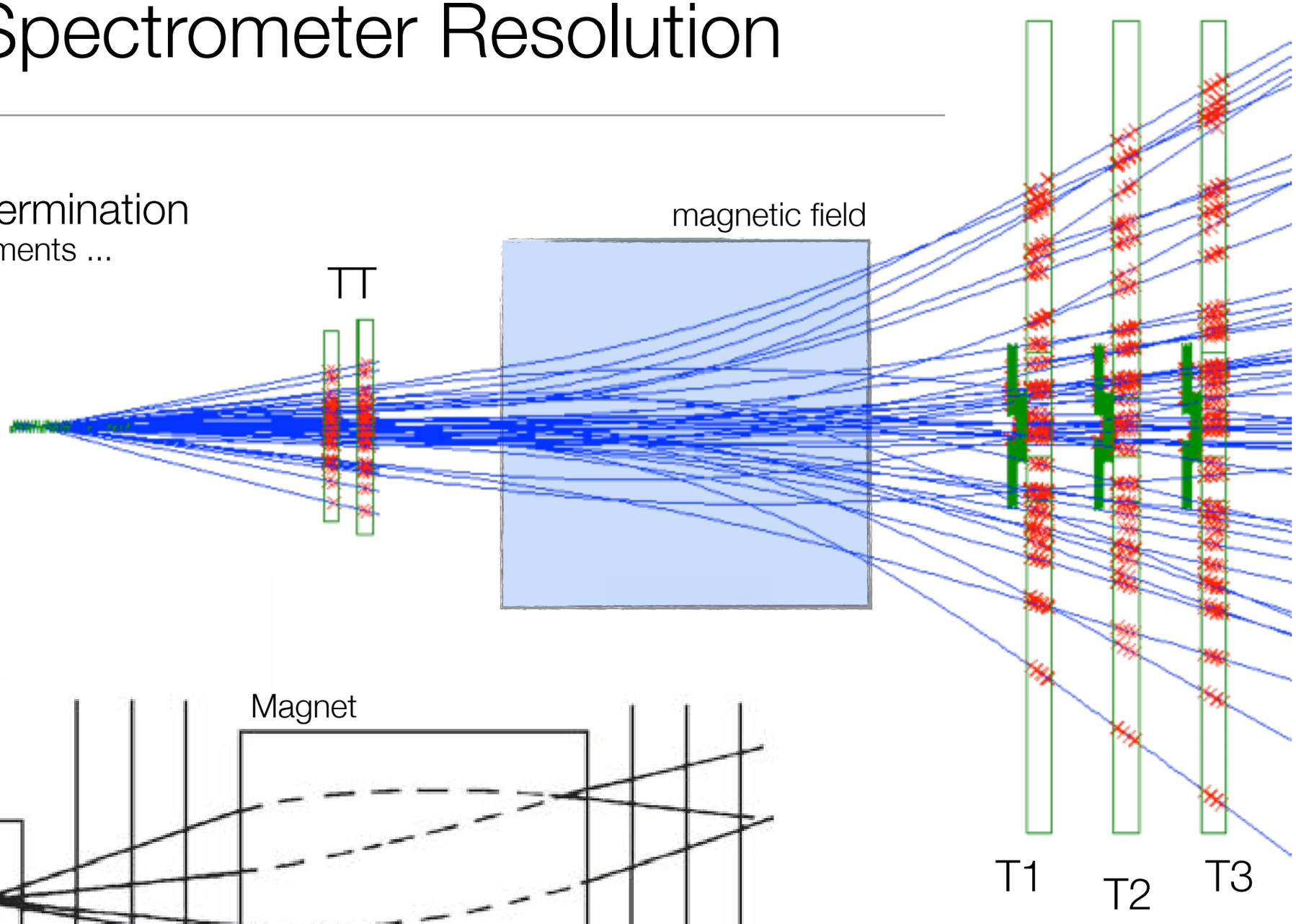

Schematics of a
Spectrometer

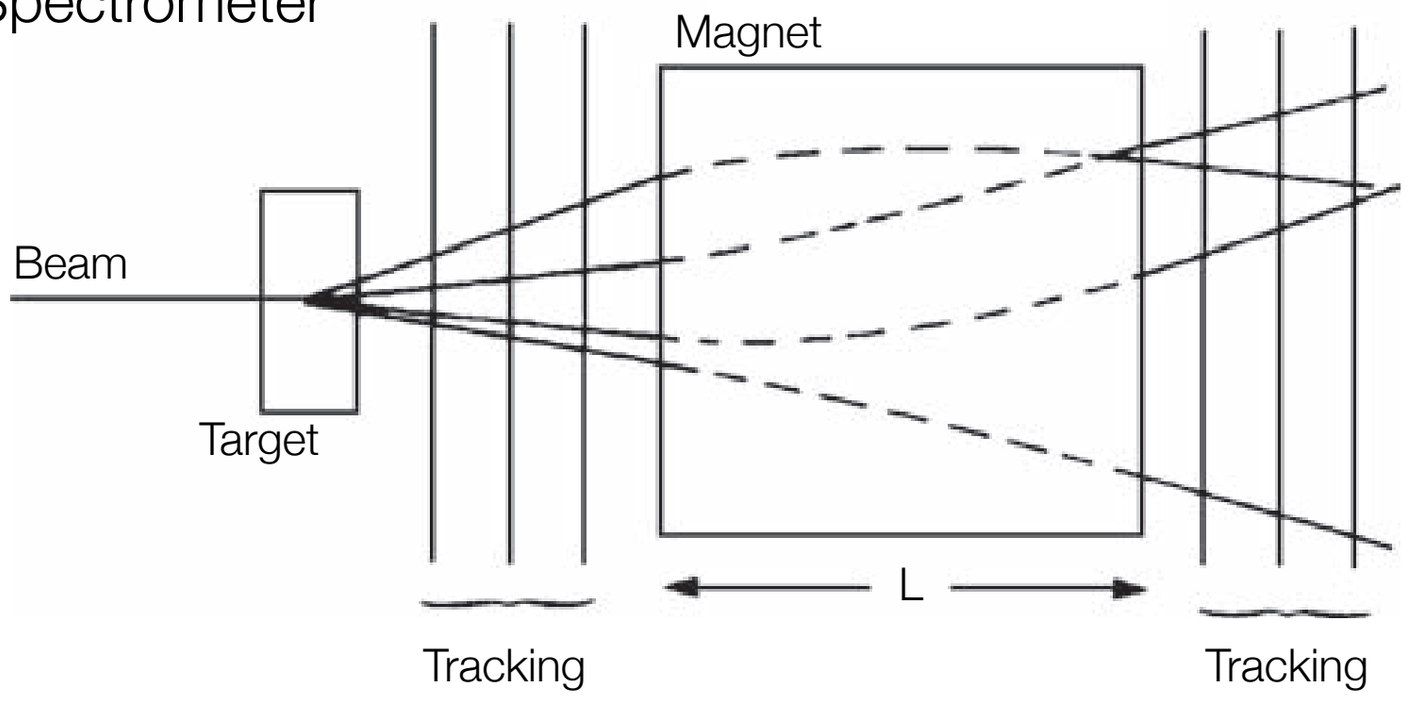

Magnetic Spectrometer Resolution

Momentum determination
in fixed target experiments ...

$$p = eRB \qquad \vartheta = {}^{L}/_{R} = {}^{L}/_{p} \cdot eB$$

$$p = eB \cdot {}^{L}/_{\vartheta}$$

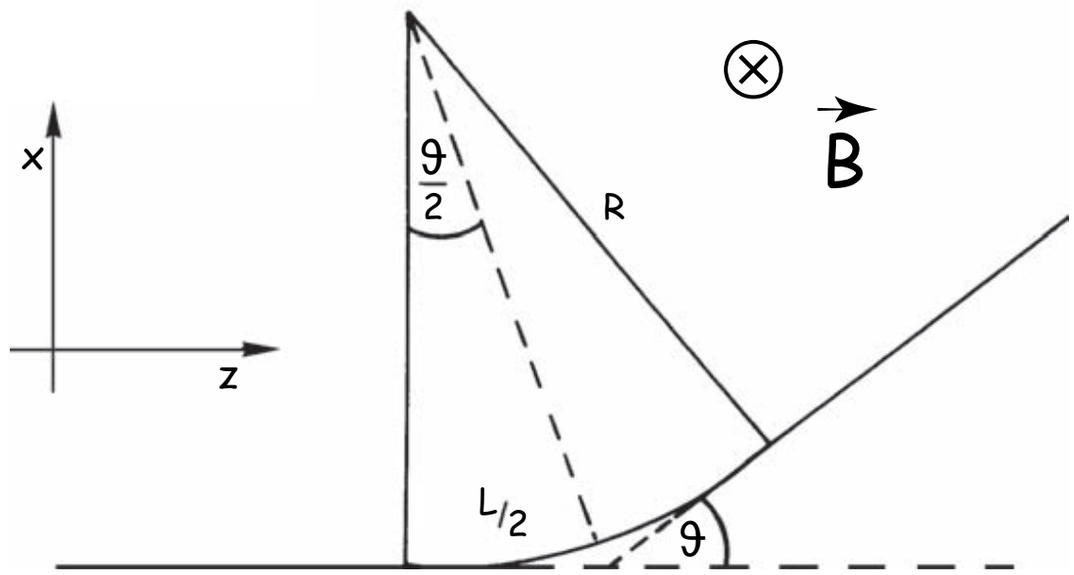

Momentum resolution:

$$\rightarrow \quad \frac{\sigma_p}{p} = \frac{\sigma_\vartheta}{\vartheta}$$

with

$$\sigma_\vartheta \sim \sigma_x$$

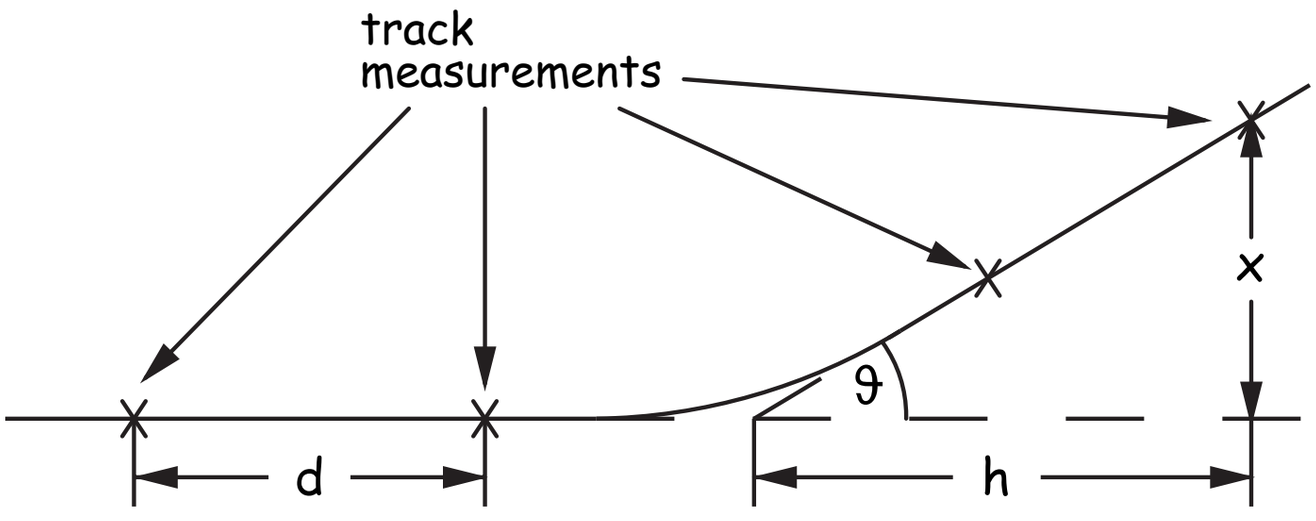

Determination of σ_p/p:

$$\vartheta = \frac{x}{h} \qquad \sigma_\vartheta = \frac{\sigma_x}{h}$$

$$\frac{\sigma_p}{p} = \frac{\sigma_\vartheta}{\vartheta} = \frac{\sigma_x}{h} \cdot \frac{p}{eBL}$$

Long lever arm improves momentum resolution ...

Drift Chambers – Ambiguities

Difficulty:

Time measurement cannot distinguish whether particle has passed right or left from a wire ...

"Left-Right Ambiguity"

Solution: "Staggered wires"

Use multiple (two) layers displaced relative to each other ...

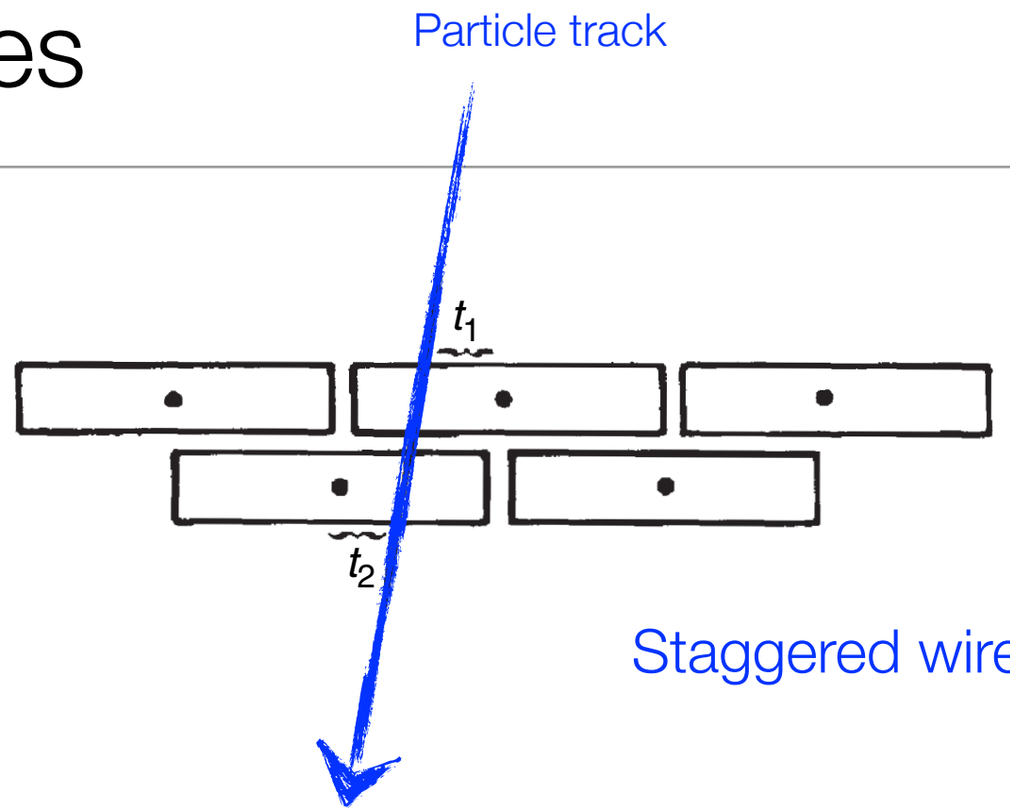

Staggered wires

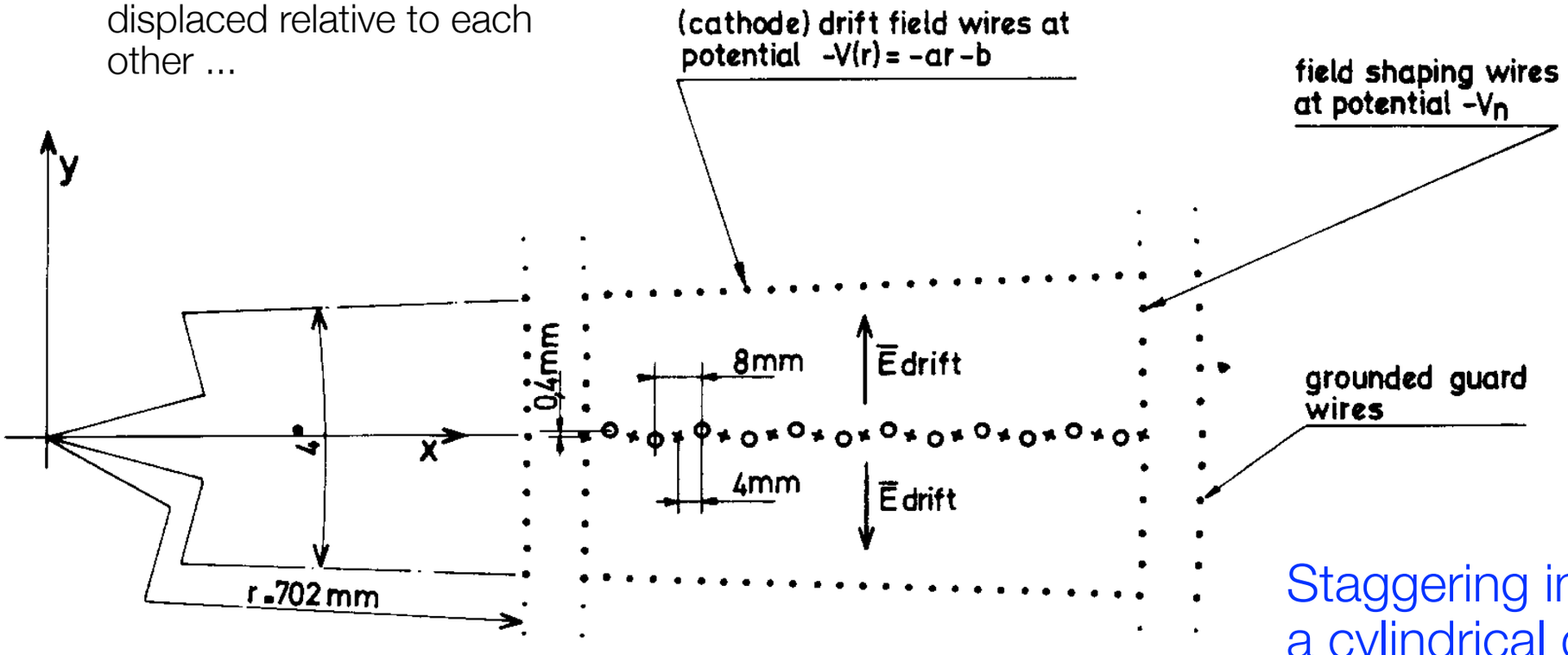

Staggering in a cylindrical drift chamber [see later]

Drift Chambers – Ambiguities

Methods to resolve
left-right ambiguities ...

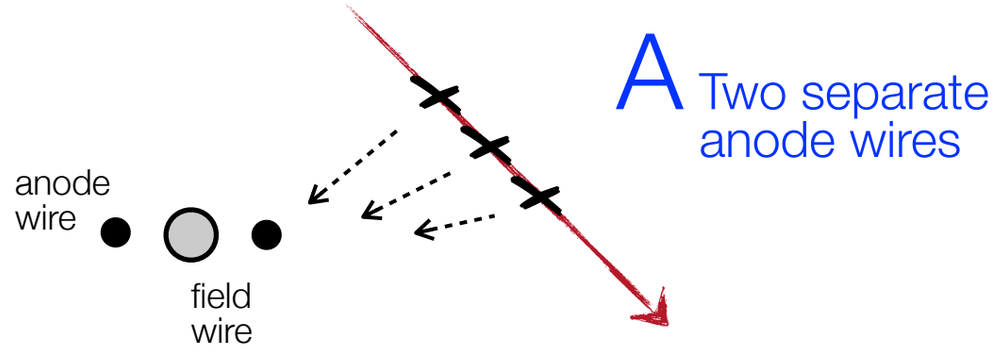

A Two separate anode wires

B Inclined anode wires

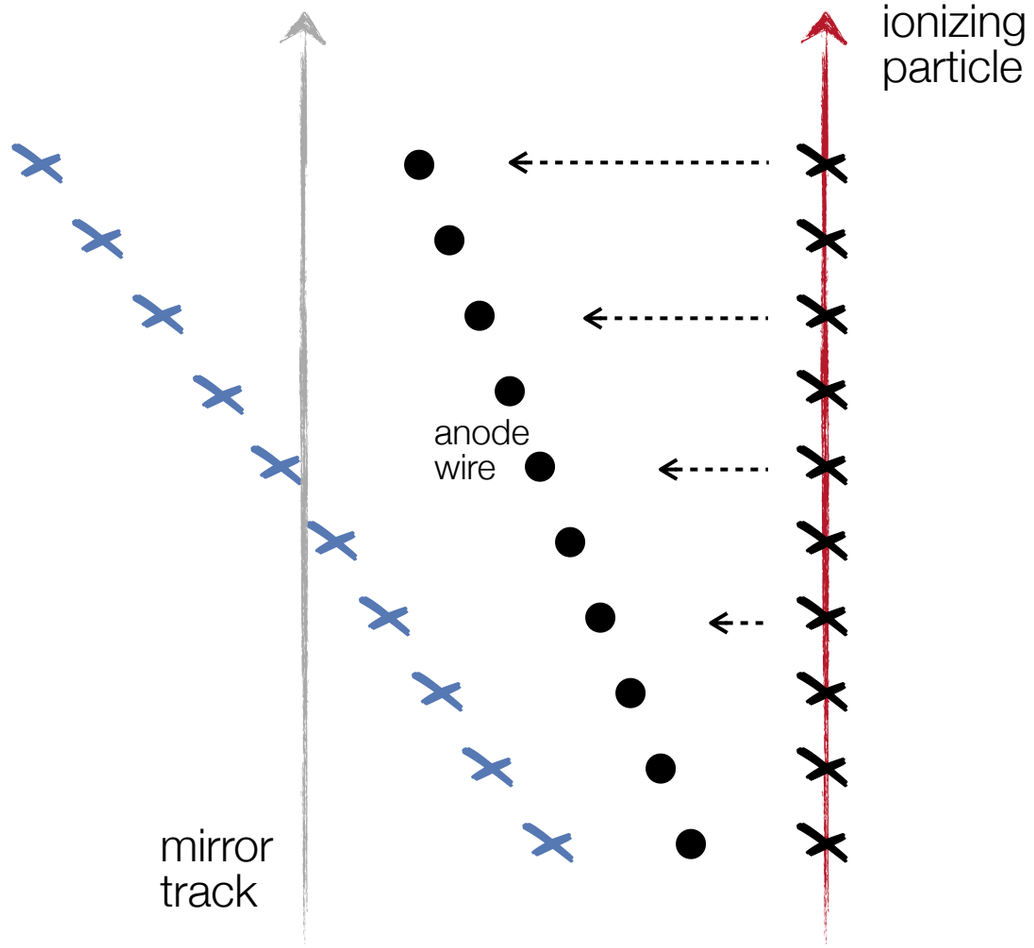

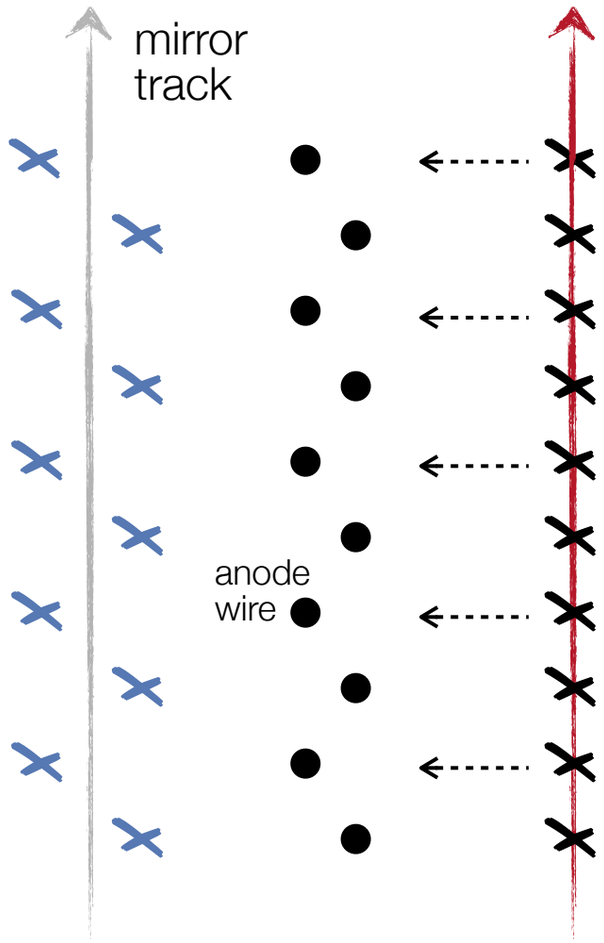

C Staggered anode wires

Aging in Wire Chambers

Avalanche formation can be considered as micro plasma discharge.

Consequences:

- Formation of radicals i.e. molecule fragments
- Polymerization yields long chains of molecules
- Polymers may be attached to the electrodes
- Reduction of gas amplification

Important:
Avoid unnecessary contamination ...

Harmful are ...

- Halogens or halogen compounds
- Silicon compounds
- Carbonates, halocarbons
- Polymers
- Oil, fat ...
- ....

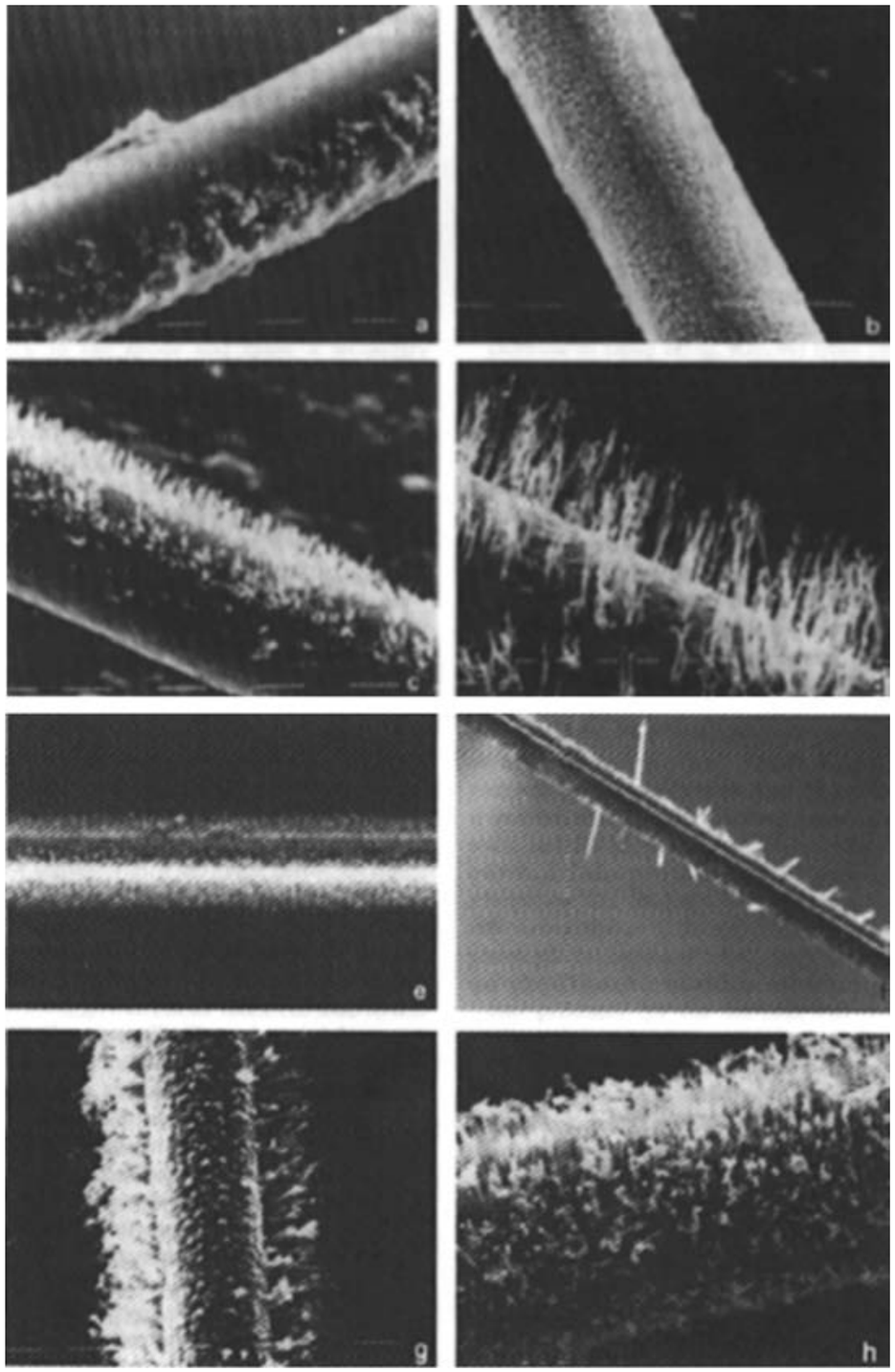

Jet Drift Chambers

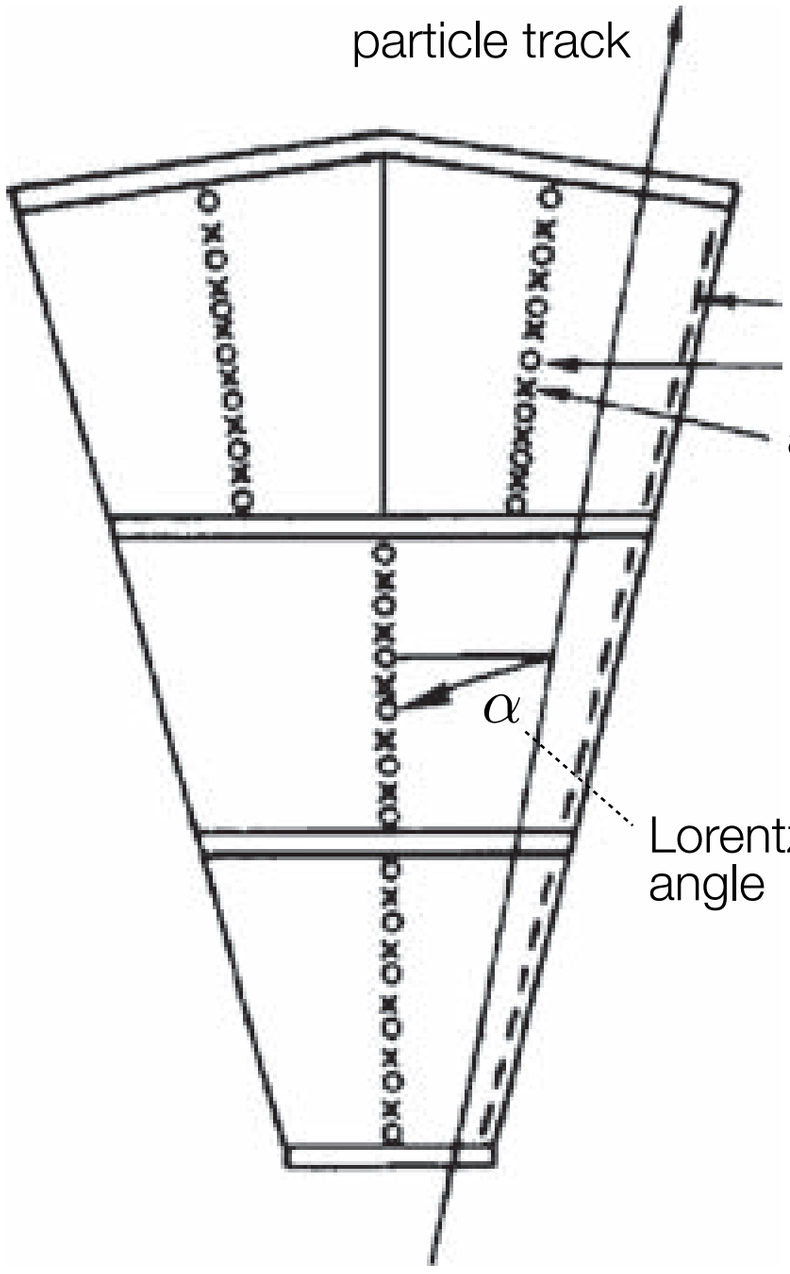

Features:

Large number of sense wires
Large drift cells

Allows good dE/dx determination
[many measurements]

But: long drift times ...

Jet Drift Chambers – JADE

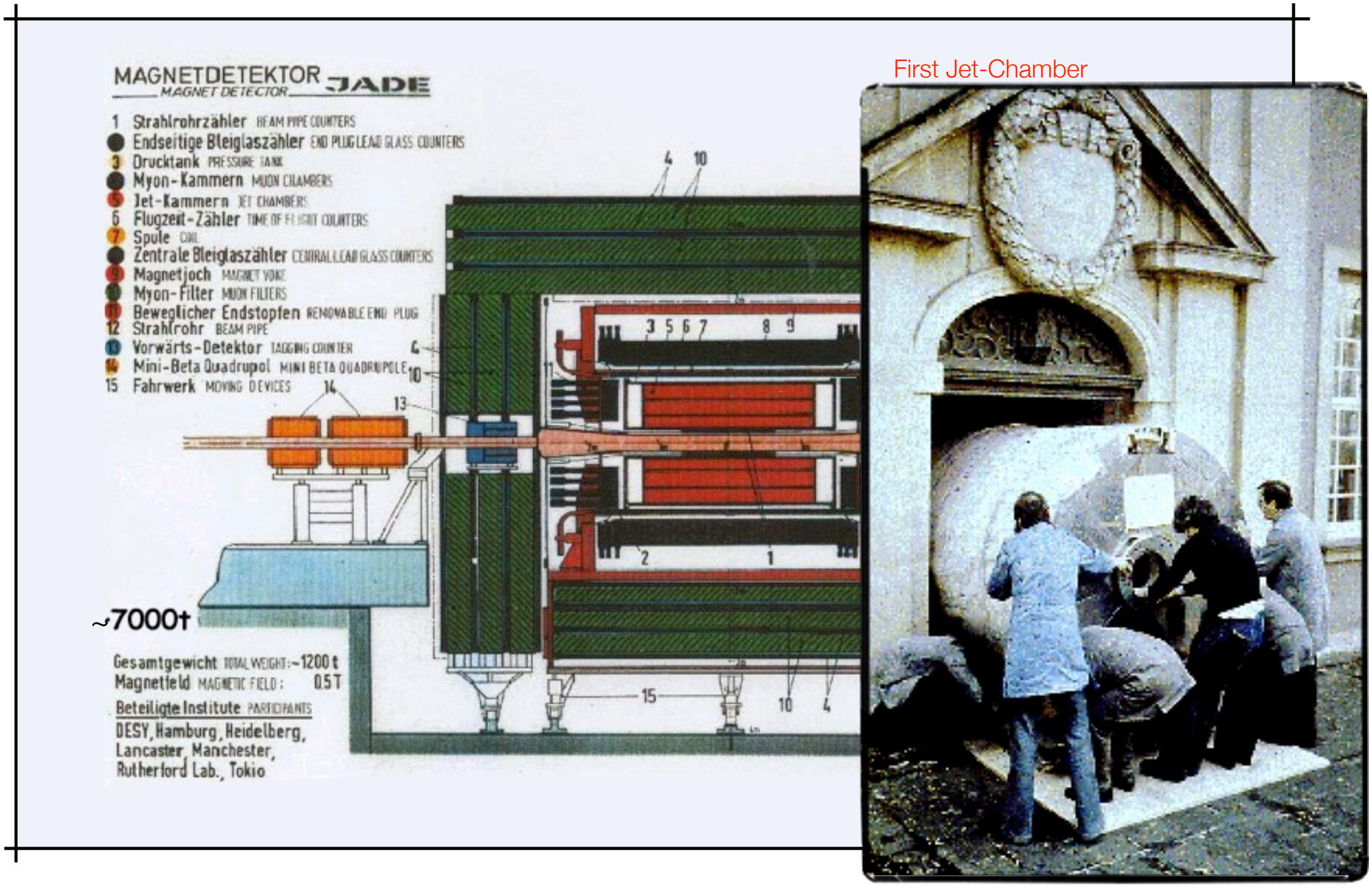

Jet Drift Chambers – JADE

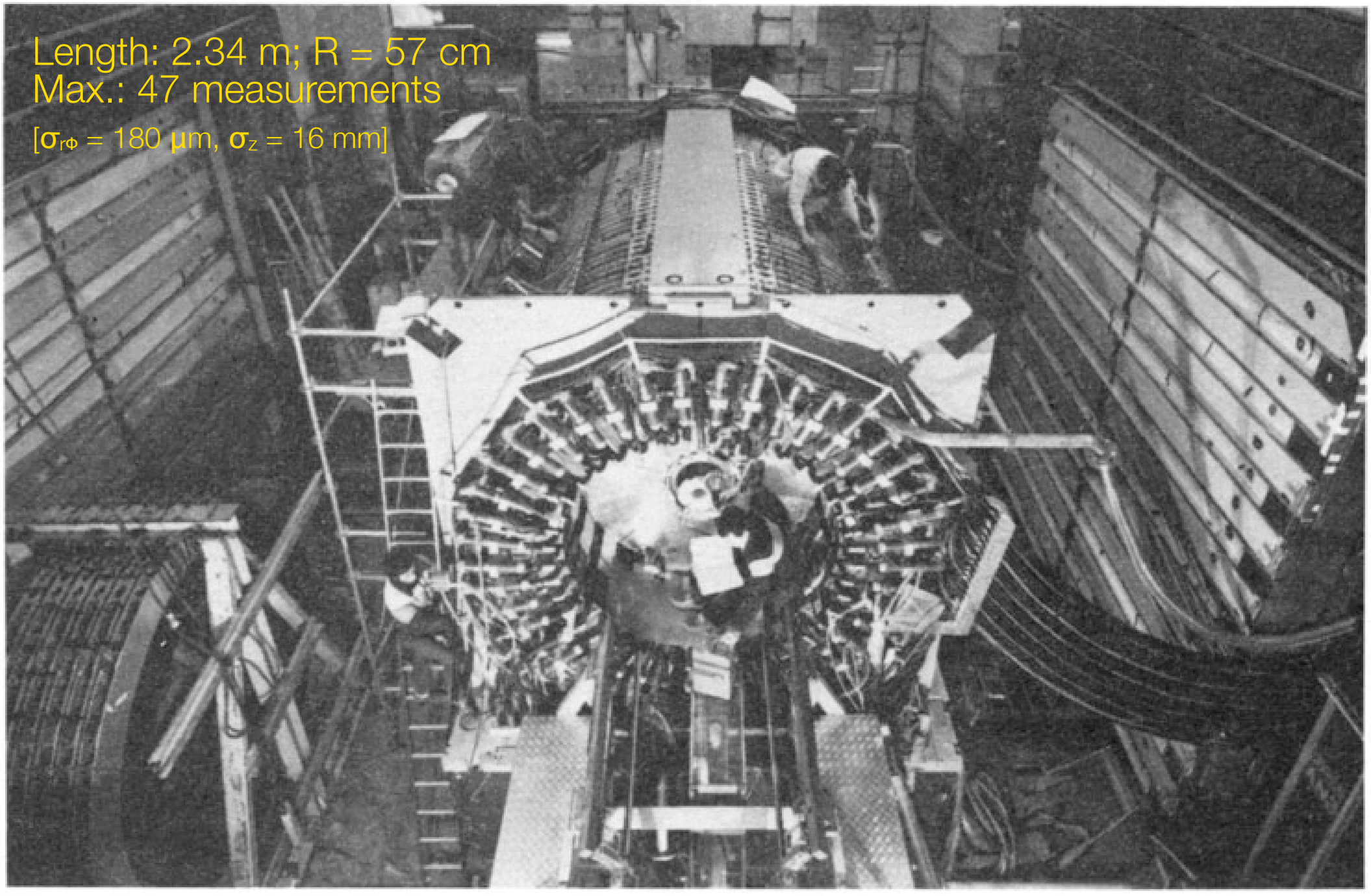

Jet Drift Chambers – JADE

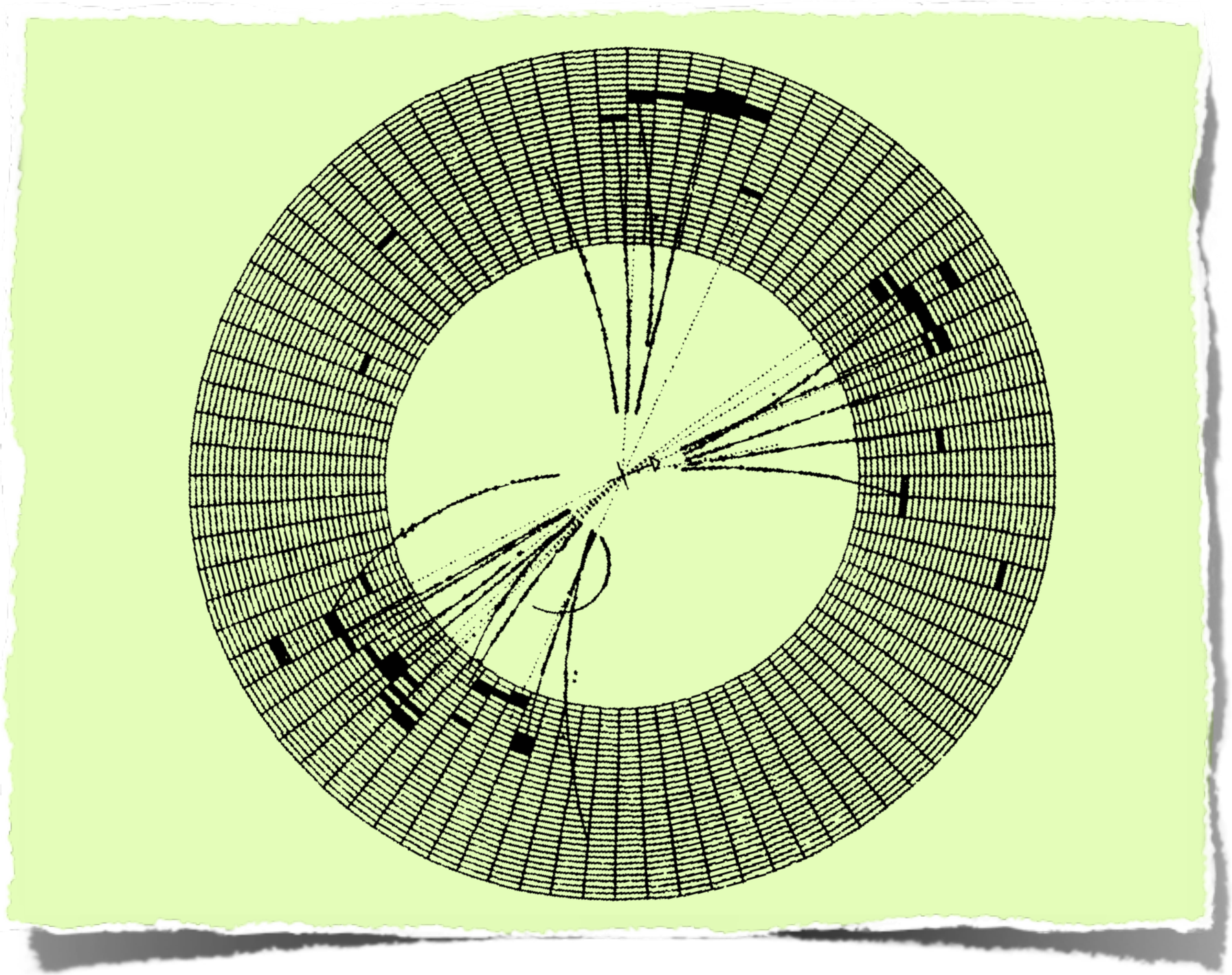

Jet Drift Chambers – JADE

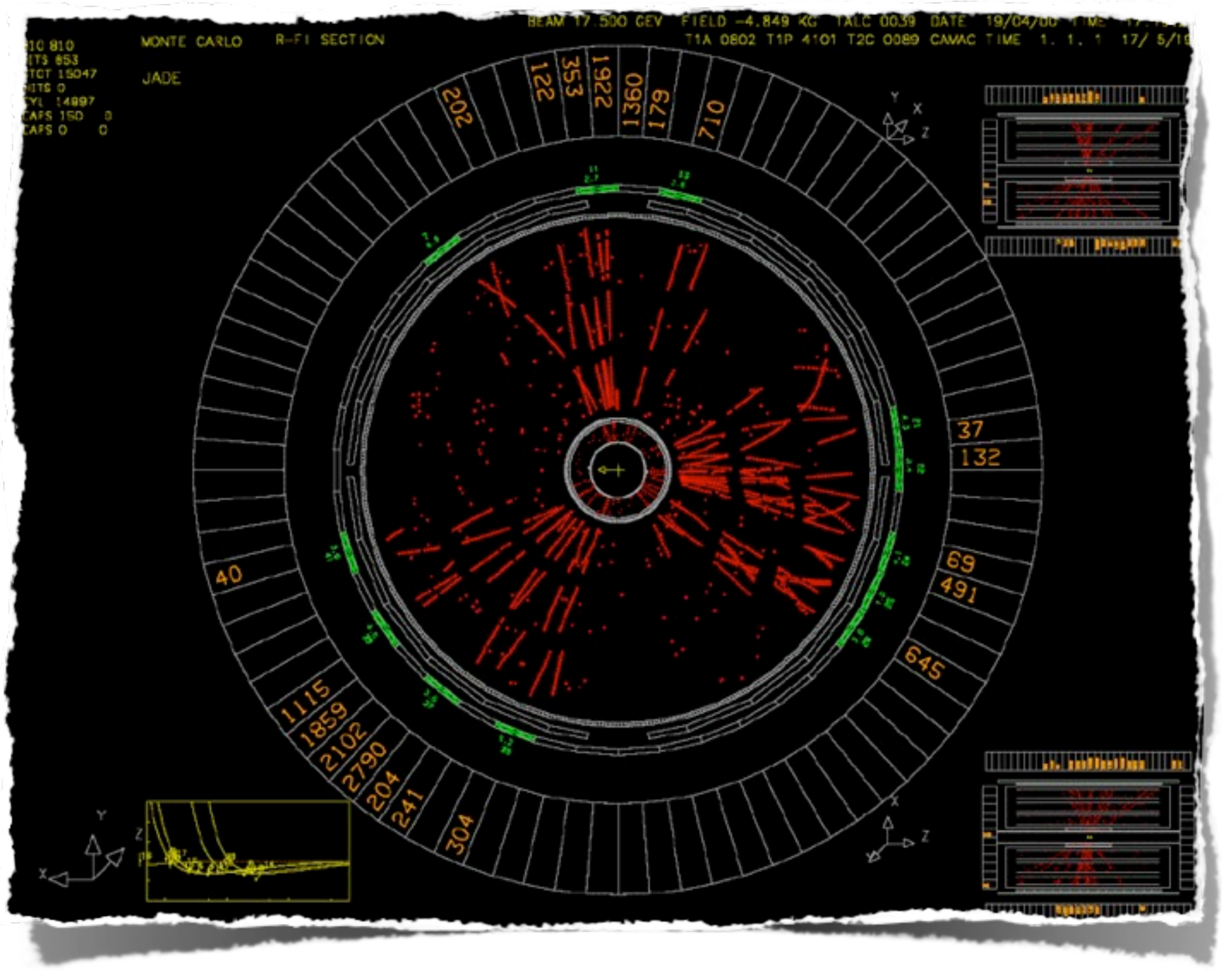

Jet Drift Chambers – JADE

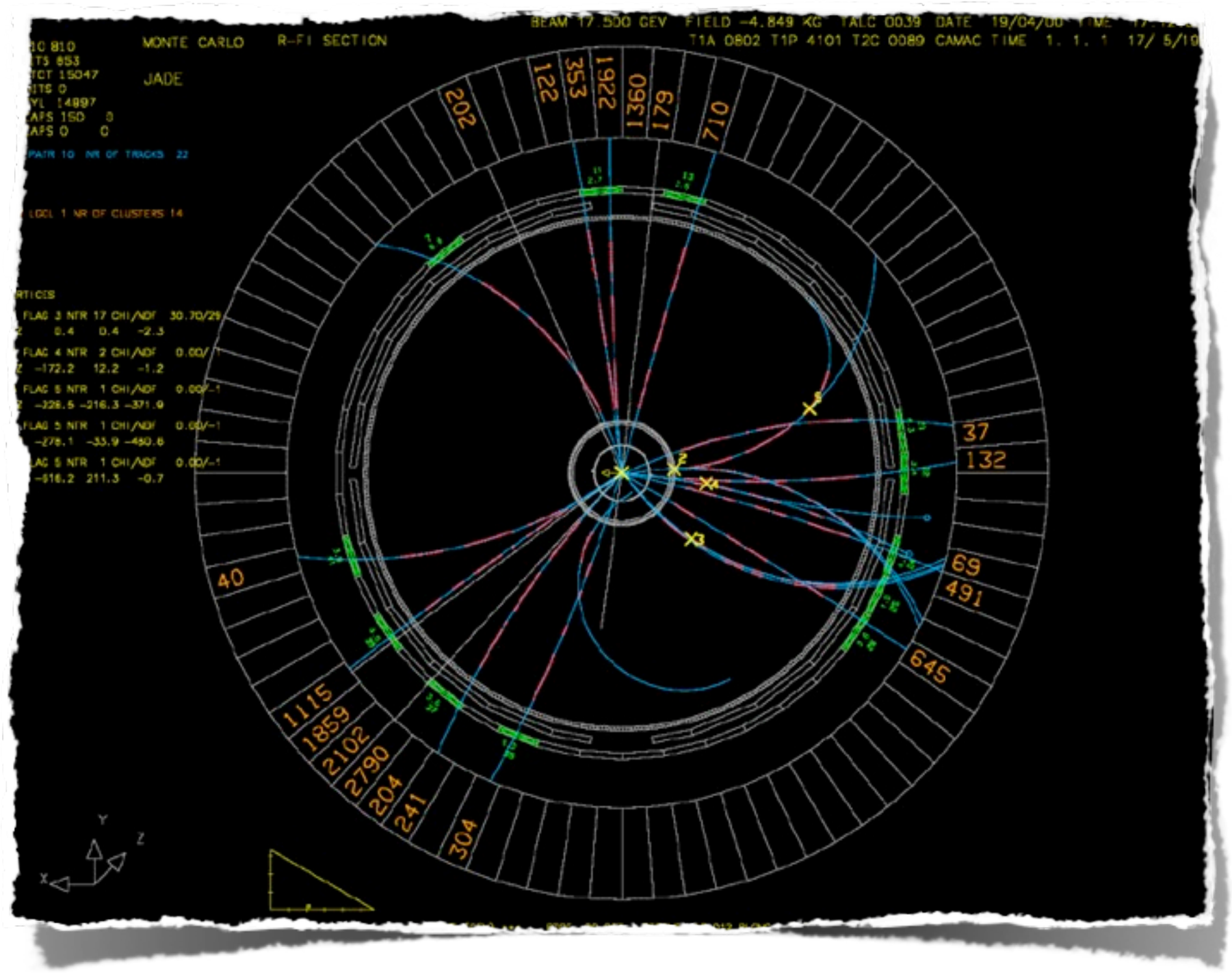

Jet Drift Chambers – OPAL

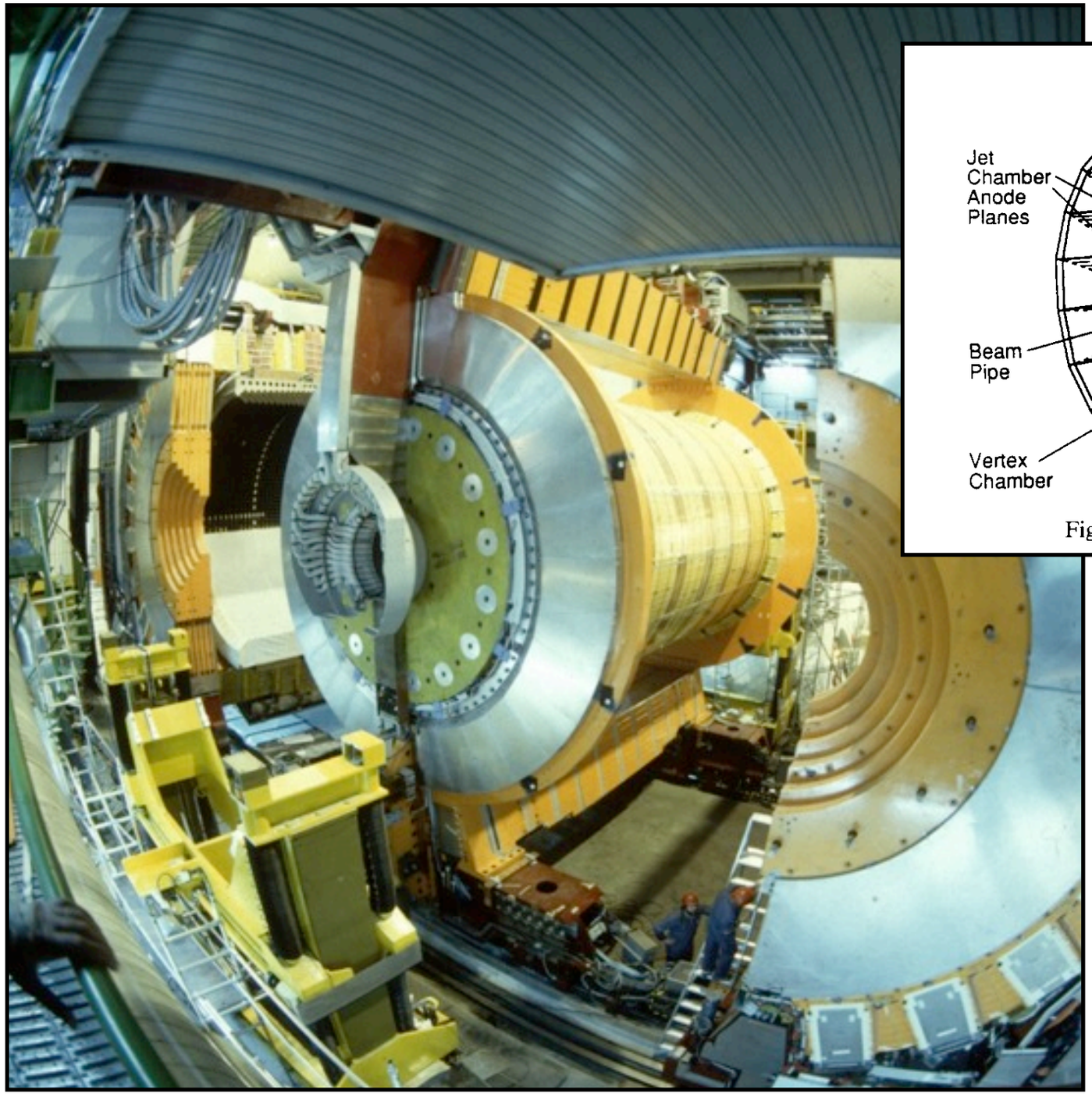

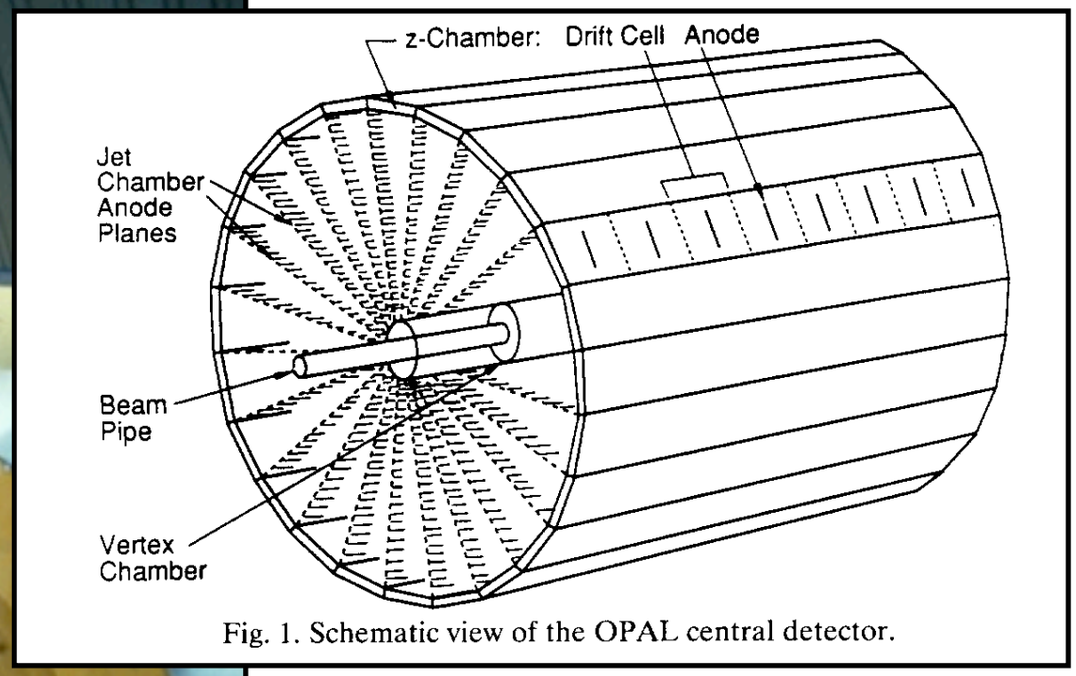

Fig. 1. Schematic view of the OPAL central detector.

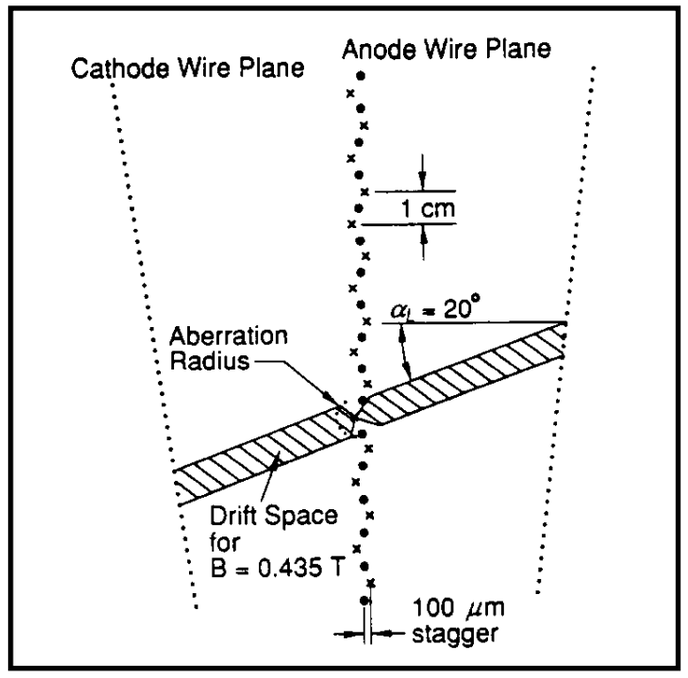

Opal Jet Chamber

Jet Drift Chambers – OPAL

Interior of OPAL drift chamber
Length: 4 m; R = 185 cm; 159 measurements per track
[$\sigma_{r\Phi}$ = 135 μm, σ_z = 60 mm]

Jet Drift Chambers – OPAL

OPAL Jet Chamber installation

Time Projection Chambers

Electronic 'bubble chamber'
Full 3D reconstruction ...

xy : from wires and pads of MWPC ...
z : from drift time measurement

Momentum measurement ...

space point measurement
plus B field ...

Energy measurement ...

via dE/dx ...

TPC setup:

(mostly) cylindrical detector

central HV cathode
MWPCs at end-caps of cylinder

B ∥ to E ➛ Lorentz angle = 0

Charge transport :

Electrons drift to end-caps

Drift distance several meters

Continuous sampling of induced charges in MWPC

TPC principle
[rz view]

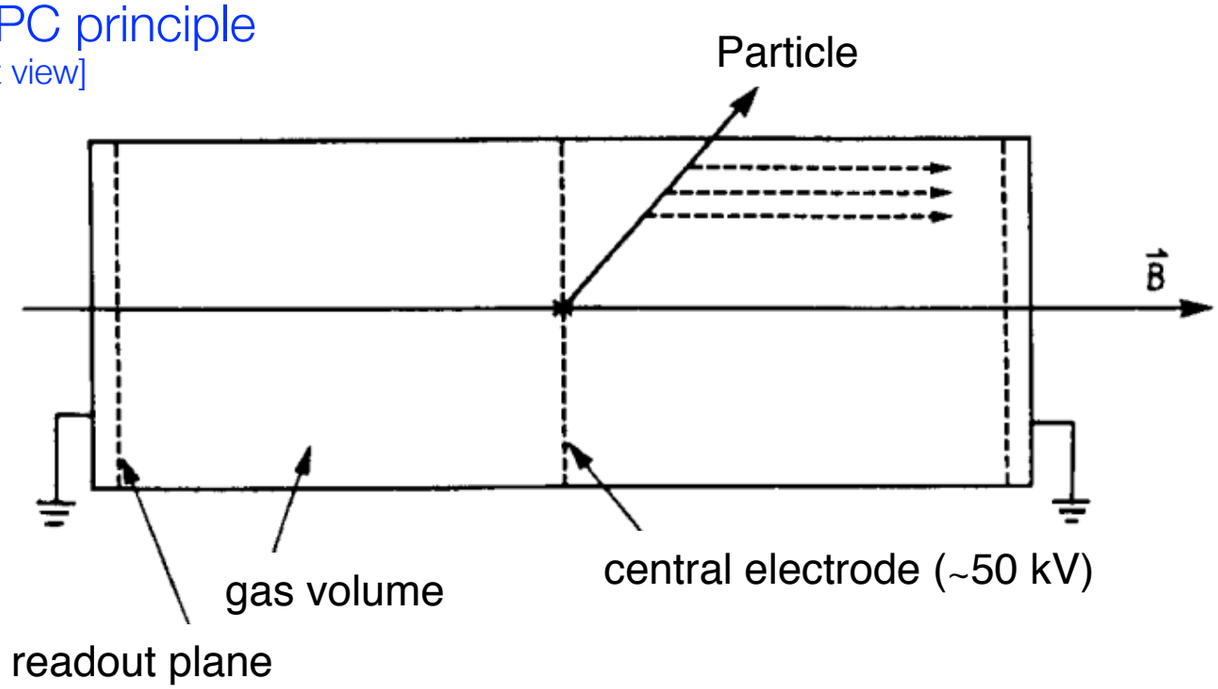

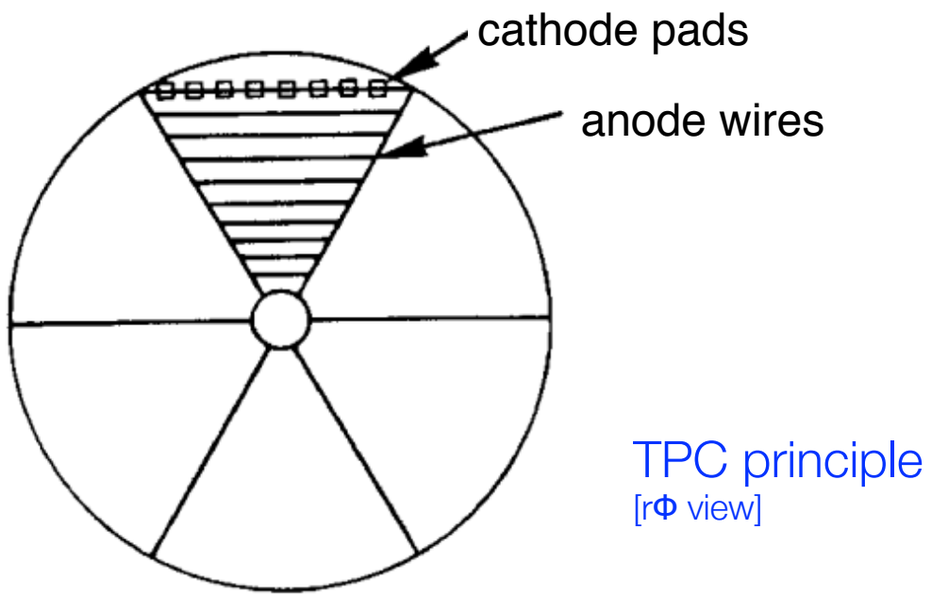

TPC principle
[rΦ view]

Time Projection Chambers

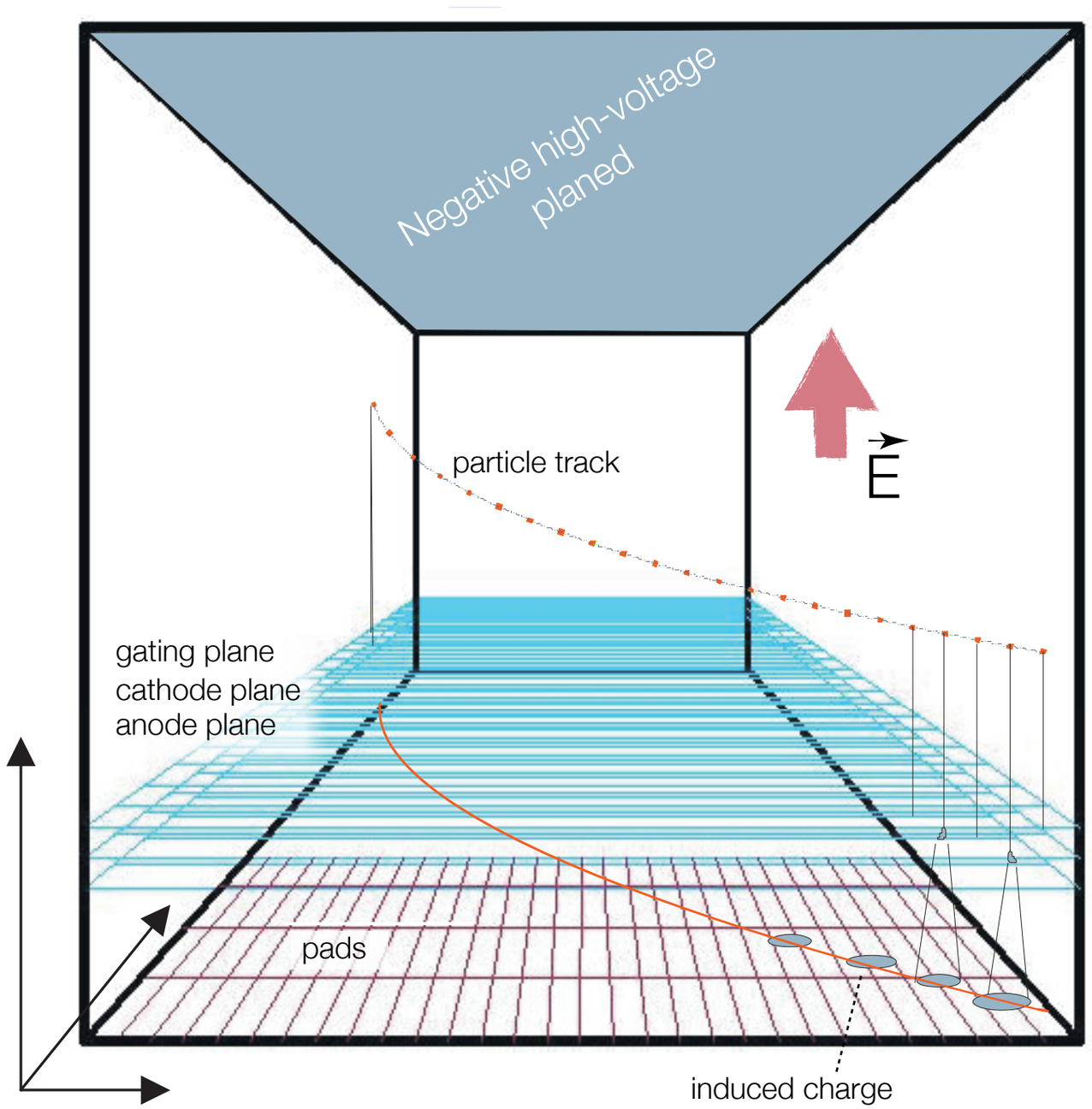

Advantages:

Complete track within one detector yields good momentum resolution

Relative few, short wires (MWPC only)

Good particle ID via dE/dx

Drift parallel to B suppresses transverse diffusion by factors 10 to 100

Challenges:

Long drift time; limited rate capability [attachment, diffusion ...]

Large volume [precision]

Large voltages [discharges]

Large data volume ...

Extreme load at high luminosity; gating grid opened for triggered events only ...

Typical resolution:

z: mm; x: 150 - 300 μm; y: mm
dE/dx: 5 - 10%

Time Projection Chambers

Difficulty: space charge effects due to slow moving ions
change effective E-field in drift region ....

Important: most ions come from amplification region

Solution: Invention of gating grid; ions drift towards grid ...

[Also: shielding grid to avoid sense wire disturbance when switching]

Requires external trigger to switch gating grid ...

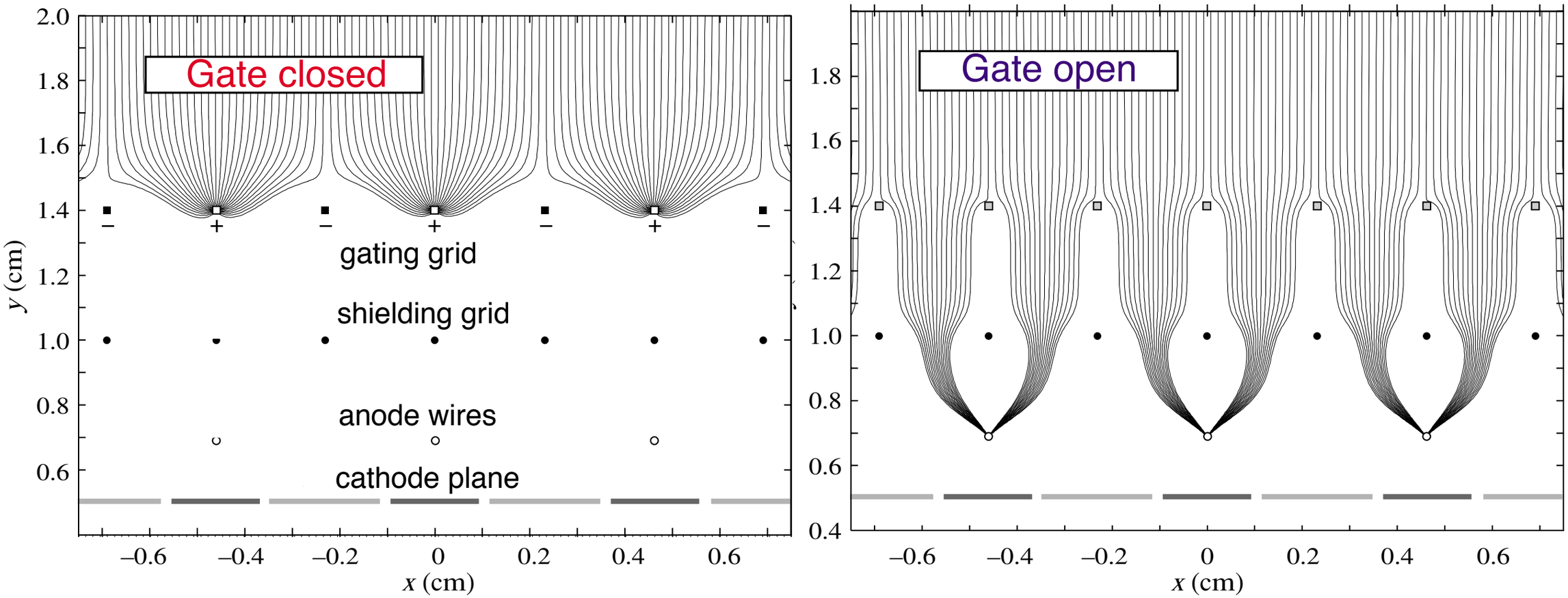

Time Projection Chambers

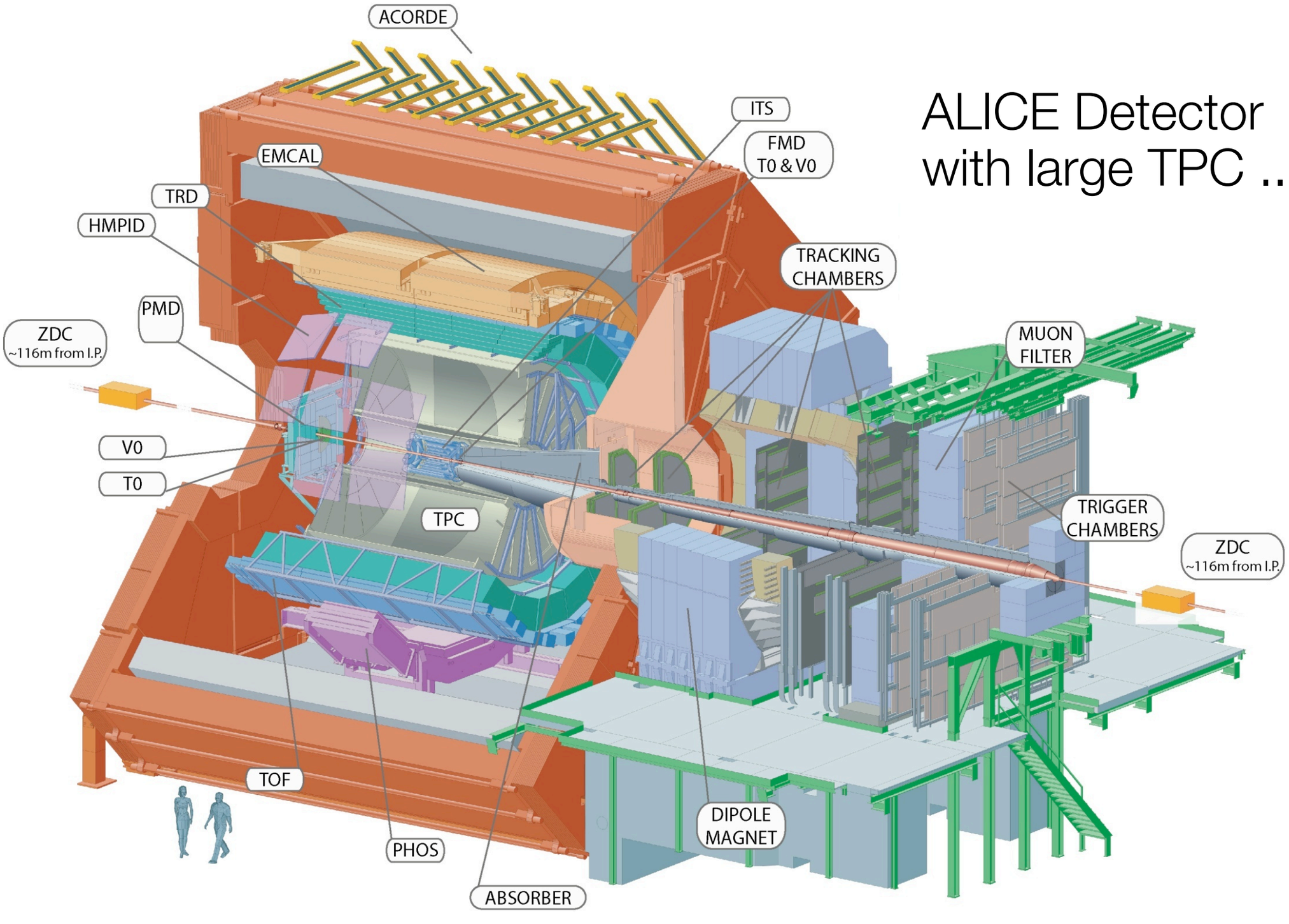

ALICE Detector
with large TPC ...

Time Projection Chambers

ALICE TPC:

Length: 5 meter
Radius: 2.5 meter
Gas volume: 88 m^3

Total drift time: 92 μs
High voltage: 100 kV

End-cap detectors: 32 m^2
Readout pads: 557568

159 samples radially
1000 samples in time

Gas: $Ne/CO_2/N_2$ (90-10-5)
Low diffusion (cold gas)

Gain: > 10^4

Diffusion: σ_t = 250 μm
Resolution: $\sigma \approx 0.2$ mm

$\sigma_p/p \sim 1\%\ p$; $\varepsilon \sim 97\%$
$\sigma_{dE/dx}/(dE/dx) \sim 6\%$

Magnetic field: 0.5 T

Pad size: 5x7.5 mm^2 (inner)
6x15 mm^2 (outer)

Temperature control: 0.1 K
[also resistors ...]

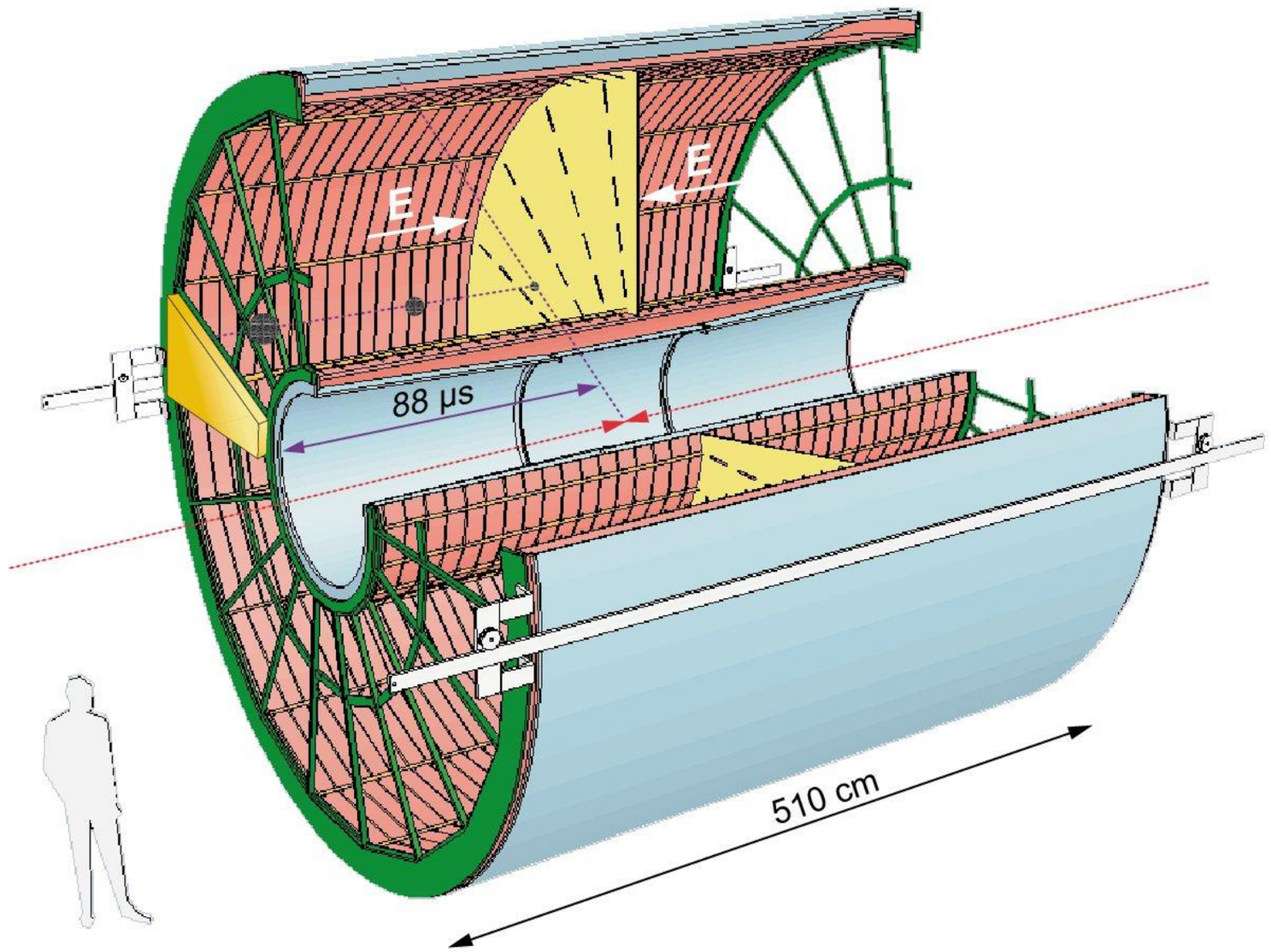

Material: Cylinder build from composite material of airline industry (X_0= ~ 3%)

Time Projection Chambers

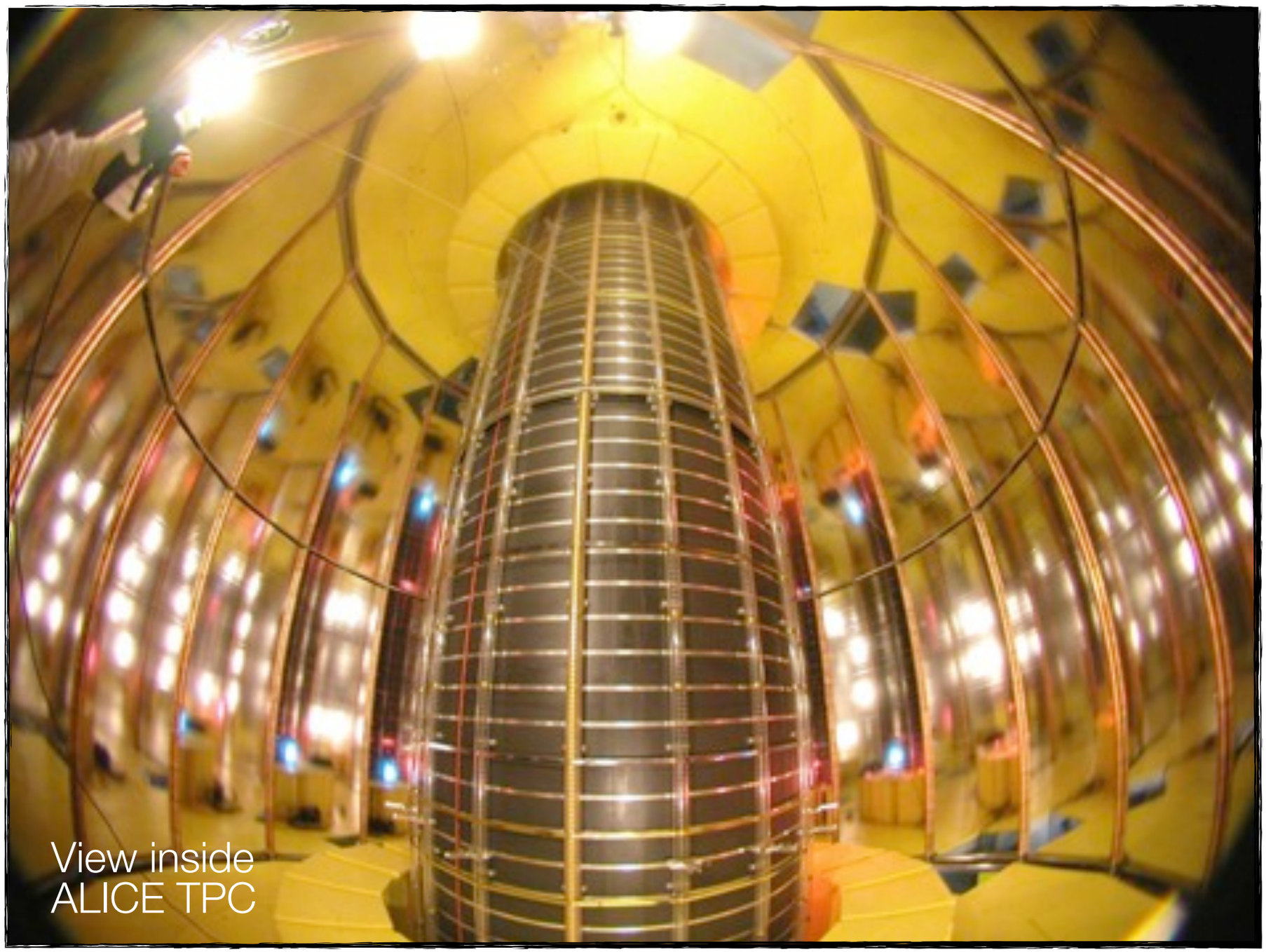

Time Projection Chambers